BTA/PE/11-06 *Underbalanced drilling operations*

Friction loss modeling of two phase annular flow.

20/05/2011 *I.L. van der Sluijs*

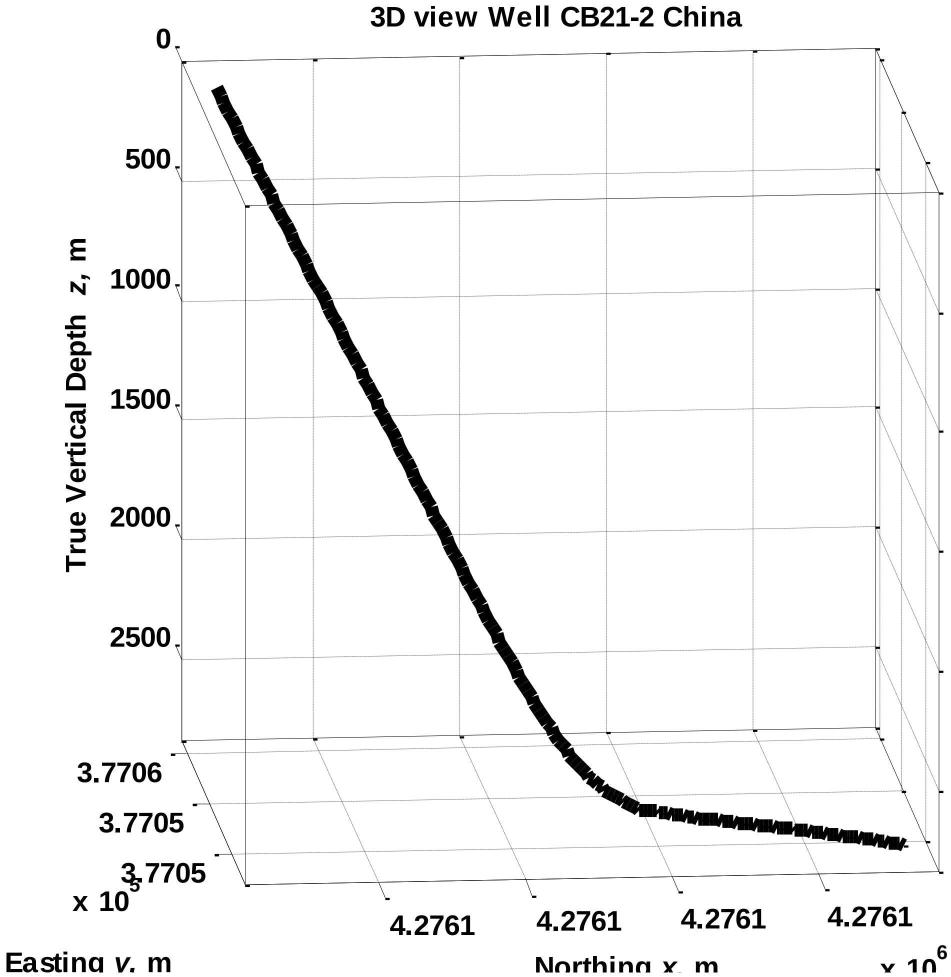

TU Delft

Department of Geotechnology

Delft University of Technology

Title	:	Underbalanced drilling operations Friction loss modeling of two phase annular flow.
Author(s)	:	I.L. van der Sluijs
Date	:	20/05/2011
Professor(s)	:	J.D. Jansen
Supervisor(s)	:	J.D. Jansen J.M. Godhavn G.L.J. de Blok
TA Report Number	:	BTA/PE/11-06
Postal Address	:	Section for Petroleum Engineering Department of Applied Earth Sciences Delft University of Technology P.O. Box 5028 The Netherlands
Telephone	:	(31) 15 2781328 (secretary)
Telefax	:	(31) 15 2781189

Preface

This bachelor thesis is conducted as part of the undersigned candidate's Bachelor of Science at the department of Geosciences at the TU Delft.

I would like to thank my supervisor Professor J.D. Jansen for good guidance and support during the project.

I would also like to thank Professor J.M. Godhavn, Norwegian University of Science and Technology and G. de Blok, Delft University of Technology for their support and feedback as well as everyone else who provided me with information during this project.

The undersigned hereby declares that the project is written solely by himself and according to the rules of the Technical University of Delft.

Delft 20 May 2011

I.L. van der Sluijs

Abstract

This project develops a software tool to model pressure loss of two phase flow in the annulus of a well during underbalanced drilling. By adjusting the Mukherjee and Brill correlation for production/injection wells, insight into which parameters are of influence in predicting the frictional pressure drop during underbalanced drilling is gained. Also the difference between the use of oil-base mud or water-base mud is presented.

Underbalanced drilling is the oldest drilling method which over the past years received new attention for bringing new life to an old reservoir. With no reservoir impairment, this method can achieve a higher recovery factor if completed 100% underbalanced.

For the success of an underbalanced drilling operation, understanding the annular frictional performance of non-Newtonian mud is crucial. This is a key factor in the development of the hydraulic program which is used in the selection of the drilling equipment. Although several simulators exist, none of them accurately predicts the pressures which are experienced in reality. In this project a power-law model for predicting frictional pressure loss in eccentric annulus is used instead of the formulas defined by Mukherjee and Brill.

After selecting the parameters that have a potential impact on the frictional pressure loss, a range for each parameter was defined and a sensitivity analysis was performed to quantify the impact due to changes in each parameter.

Table of contents

List of figures

List of tables

1. Introduction to underbalanced drilling

1.1. Definition

Underbalanced drilling operations (UBD) can be defined as a type of well operation in which the bottom hole pressure is intentionally lower than the pore pressures of the formations exposed in the borehole, see Figure 1. Thereby, formation fluids are intentionally allowed to flow to the surface while drilling, see Figure 1. At the surface the formation fluids will be separated from the drilling fluid/gas by a continuous process. (Eck-Olsen, 2010)

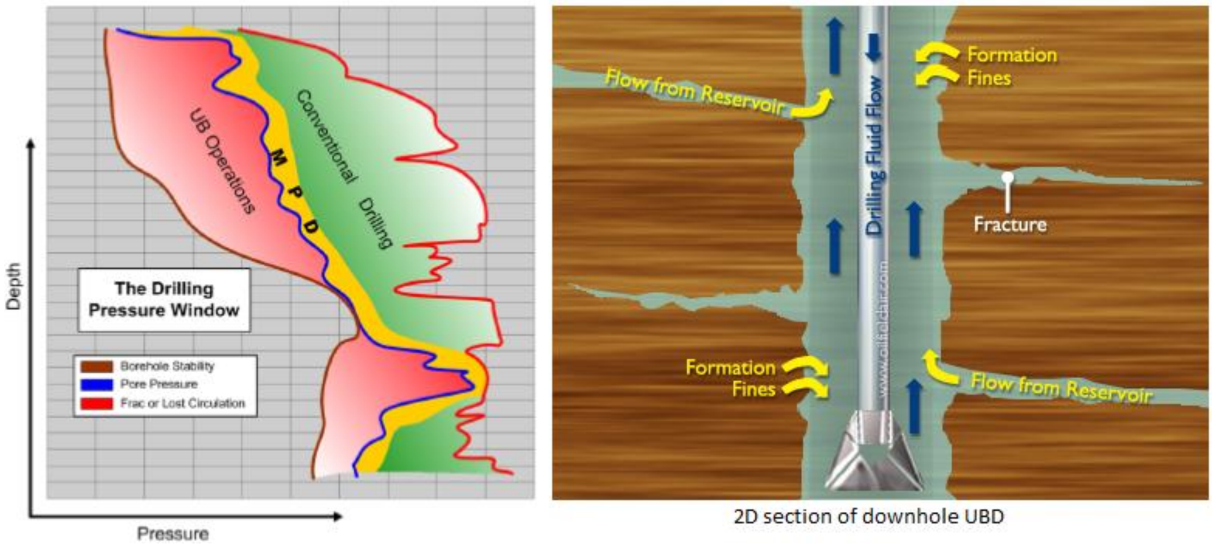

Figure 1: Overview Underbalanced Drilling (Eck-Olsen, 2003) & (Airdrilling, 2005)

1.2. History

After Colonel Drake spudded his first well in 1854, the oil usually blew out of the hole creating a large oil fountain due to underbalanced conditions, see Figure 2. Later on environmental concerns and the invention of the BOP made it possible to drill in an overbalanced state, preventing uncontrolled flow of oil to the surface. Underbalanced drilling was later on given new life when used for the re-development of fields where depleted pressure was an important concern and to drill quicker through very abrasive rocks. Nowadays UBD and Managed pressure drilling(MPD) receive a lot of attention due to the ability to automate the process, minimize reservoir impairment and increase the recovery factor(RF).

Figure 2: Lucas Gusher well, year 1901 in Spindletop, Texas (Institution)

1.3. Benefits and disadvantages

1.3.1. Benefits

The following benefits with UBD exist (Bennion, Thomas, Bietz, & Bennion, 2002):

- *Less/no formation damage:* Formations are susceptible to different types of formation damage during traditional overbalanced drilling operations, see points below. With UBD these can be mitigated and a higher Recovery Factor can be achieved. See Figure 3.

  1. Invasion of mud particles from the mud system into the formation matrix due to a badly designed filter cake or high overbalance.
  2. High-permeability zones are a potential treat for severe mud system losses

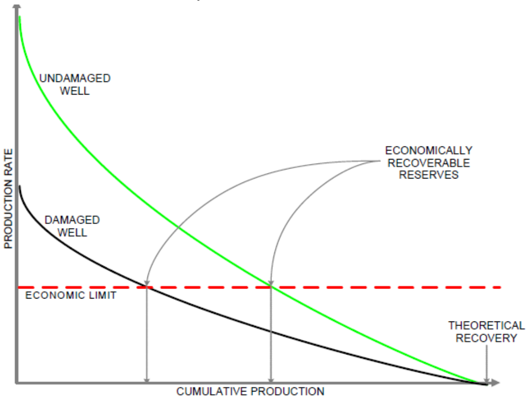

Figure 3: Reserves OBD & UBD (Qutob, 2007-2008)

- *Increased Rate of Penetration (ROP):* ROP increases due to the differential pressure created with the formation. This causes cuttings to be forced away from the borehole wall (preventing accumulation) and away from the bit face (preventing re-drilling and grinding of cuttings) thereby not only increasing ROP but also extending bit life. See Figure 4

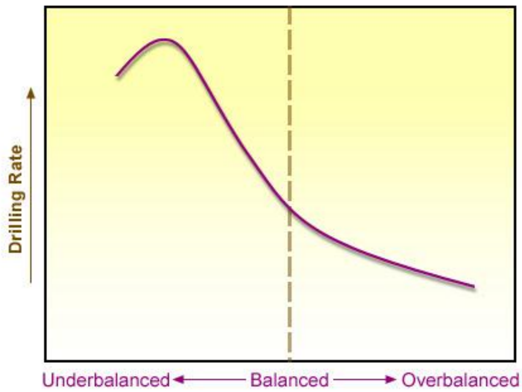

Figure 4: Drilling rate versus differential pressure in the borehole (IHRDC)

- *Eliminates some drilling problems:*

  1. No differential sticking. Since the formation has a higher pressure than the borehole, no filter cake is formed and the pressure difference between the two pushes the drill pipe away from the borehole wall.
  2. No circulation loss

- *Reservoir characterization:* Since underbalanced drilling allows hydrocarbons to flow to the surface, proper monitoring of the produced fluids at the surface can provide a good indication of productive zones of the reservoir and can be a valuable aid in geo-steering of the well.

- *Ability to flow/well test while drilling:* It is possible to conduct either single or multi-rate drawdown tests to evaluate the productive capacity of the formation and formation properties while drilling underbalanced.

- *Ability to drill depleted reservoirs where no or a small drilling window is present*

1.3.2. Disadvantages

Before performing an UBD program it is important to have a proper understanding of some of the potential downsides of the method. (Bennion, Thomas, Bietz, & Bennion, 2002)

- *Expensive:* A typical UBD program is more expensive than a traditional program due to the requirement of different surface equipment (4-phase separator, rotating control head (RCH), choke manifold) and training of personnel. For some drilling projects an additional rig pump, snubbing unit or lubricator (North Sea) is required. If the well is 100% completed underbalanced, well productivity is increased and a lower abandonment pressure can be achieved. Whether the cost of implementing the method outpaces the gain is well dependent . See Figure 5.

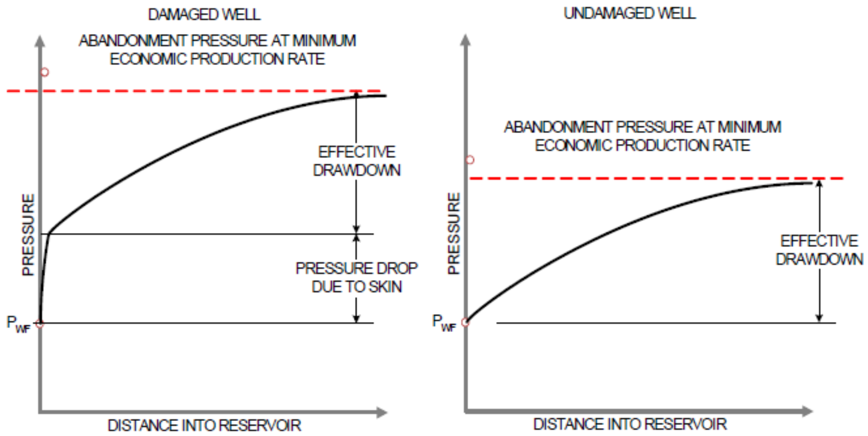

Figure 5: Damaged and Undamaged well (Qutob, 2007-2008)

- *Safety concerns:* In traditional drilling programs the heavy mud column acts as the primary well control. With UBD, the primary well control is the RCH and the emergency shut-in device (ESD) below the rig floor which would require a high a level of risk management. Care must be taken and personnel needs to be well trained.

- *Wellbore stability:* The main reason for failure of UBD operations is due to wellbore collapse particularly in poorly consolidated or highly depleted reservoirs. Sufficient geological knowledge of the underground is a necessity before starting an UB operation.

- *Failure of maintaining underbalanced condition:* If an underbalanced condition abruptly or gradually changes to an overbalanced condition, very rapid and severe invasion of filtrate and associated solids may occur. This problem gets worse since very thin, low viscosity, mud systems are usually used in UBD operations for separation purposes.

1.4. Pressure control

A successful UBD process depends on accurate modelling of multiphase flow through the drill string and the annulus. This project focused on two-phase flow through the annulus. In order to control an UBD operation it is necessary to estimate the BHP so that it remains below the pore pressure exposed by the formation.

When circulating during underbalanced drilling, the BHP is governed by a combination of fluid/gas density; the backpressure applied on top of the fluid/gas column; the frictional pressure loss of the flow and acceleration of the multiphase flow. See equation 1.4.1. Other minor contributors are pipe rotation and cuttings which both increase the friction.

1.4.1 $$P_{bottomhole} = P_{hydrostatic} + P_{choke} + P_{friction} + P_{acceleration}$$

Since frictional pressure loss is highly depended on the amount of gas(nitrogen, hydrocarbon, etc.) that flows into the annulus, it is extremely important to measure this at the surface. By putting a pressure while drilling(PWD) tool in the BHA, pressures experienced in the annulus can be measured. The hydraulic model can be adjusted with these measurement so that the actual BHP can be calculated. The control system can then by adjusting the choke make sure it stays below the pore pressure.

A sufficient geological understanding of the underground and type of formation fluids/gasses is required to properly design and model a multiphase-flow circulating system. (Saponja, 2002)

1.5. Type of drilling fluids

Drilling fluid selection is a complex but important step in the design of an UBD well. There are five main categories based primarily on the equivalent circulating density(ECD). ECD is the effective density exerted by a circulating drilling mud that takes into account the pressure drop in the annulus. (Aadnoy, Cooper, Miska, Mitchel, & Payne, 2009)

1. *Gas:* a dry gas is used as the drilling medium. Different gases are: nitrogen, natural gas, or exhaust gas.
2. *Mist:* gas drilling with up to 2.5 volume% of liquid content.
3. *Foam:* drilling with a homogeneous emulsion obtained by mixing liquid, gas and an emulsifying agent. Foam contains 55 to 97 volume% gas.
4. *Gasified liquid:* Injecting of gas into a fluid column can lower the BHP. The fluid system can be water, crude oil, diesel, water-based or oil-based mud.
5. *Liquid:* single-phase fluids only used when formation pressures are high enough

1.6. Methods to achieve an underbalanced condition

Different kinds of methods exist to achieve the required BHP such as:

- Standpipe injection: A mixture of gas and liquid is pumped through the drill pipe and mixes with the formation fluids/gasses. Typical mixtures of gas/liquid are discussed in chapter 1.5, point 2,3 and 4. See Figure 6a for a schematic.
- Flow drilling: A single-phase gas or liquid is pumped through the drill pipe and mixes with the formation fluids/gasses. Typical gasses or fluids used are discussed in chapter 1.5, point 1 and 5. See Figure 6b for a schematic.
- Micro-annulus injection: A type of underbalanced drilling in which no medium is pumped through the drill pipe but a gas discussed in chapter 1.5, point 1, is halfway injected through an intermediate casing string or parasite string. See Figure 6c for a schematic.

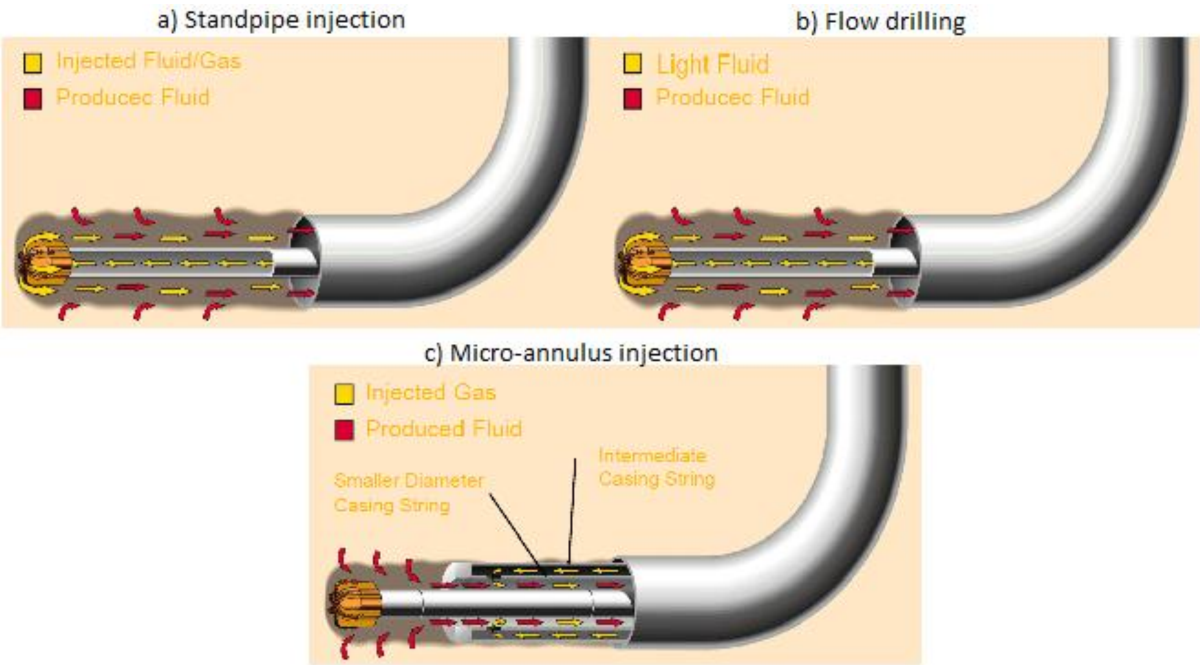

Figure 6: Different UB Methods (Eck-Olsen, 2010)

2. Hydraulics

In underbalanced operations the mud system consists of a gas, liquid and solid phase. Managing both this diverse mud system out of the well and the down hole pressure is the key to a successful UBD operation. Variables affecting the down hole pressure as well as the flow rate out of the well are subject to variations making the mud system very dynamic. Dynamic computer simulation can improve engineering design and the execution.

Pressure loss due to friction is very sensitive to changes in the operational parameters as will be shown in the sensitivity analysis and is therefore the key factor in dynamic modelling. (Lage, Fjelde, & Time, 2000)

2.1. Flow patterns

In two-phase flow systems there exist different flow patterns. The existence of a particular flow pattern is dependent on the flow rate, fluid properties and size of the annular flow path. The reason to distinguish between the flow patterns is that each flow pattern has its own set of formulas to calculate liquid holdup and the total pressure gradient. In this project the Mukherjee and Brill model is used to evaluate the flow patterns and calculate the pressure gradient (Brill & Mukherjee, 1999). In figure 7 the different flow patterns that can exist in this model are presented.

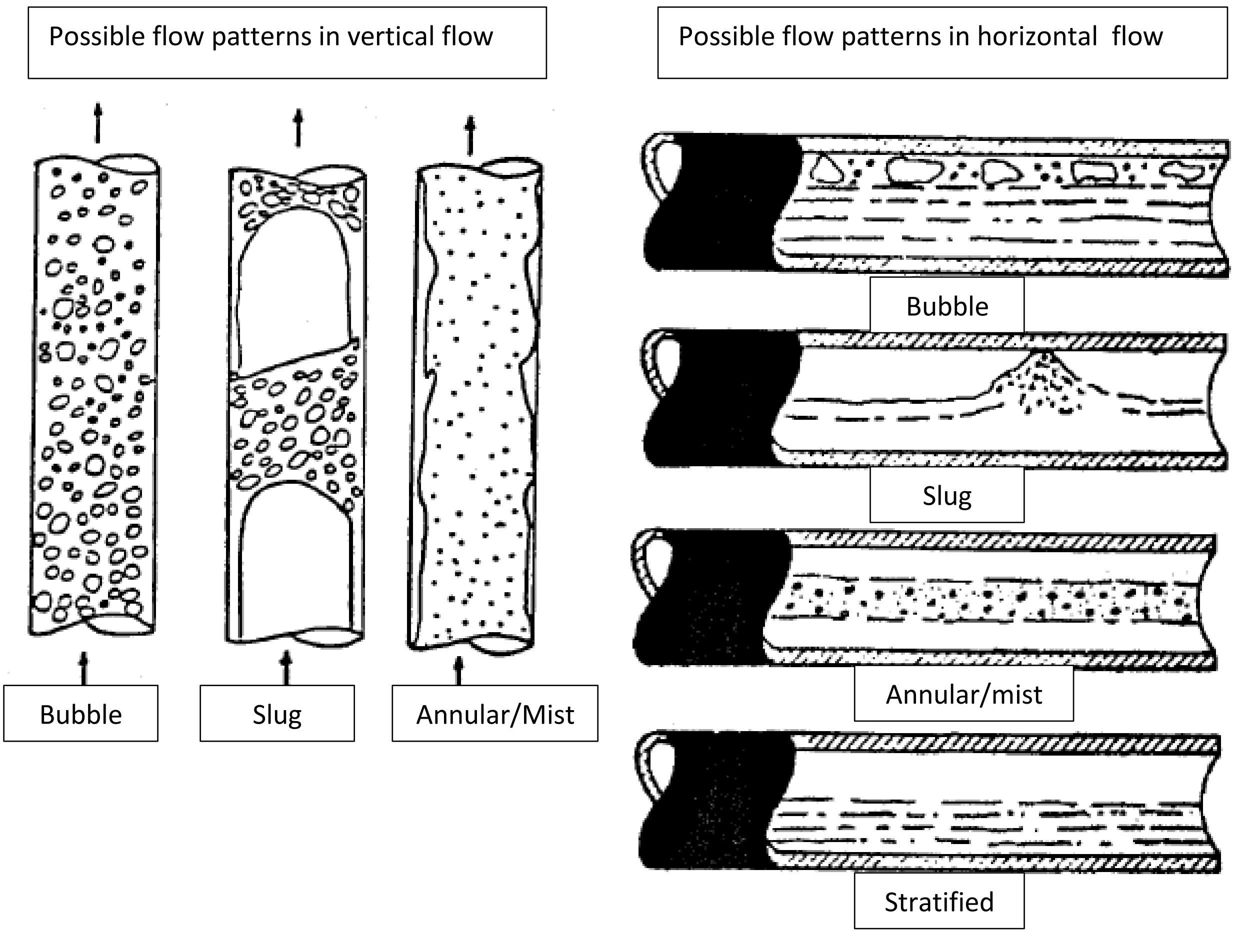

Figure 7: Flow patterns (Brill & Mukherjee, 1999)

2.2. Mukherjee and Brill method

Pérez-Téllez, Smith, & Edwards, (2002) stated that the Beggs and Brill correlation was the most popular among commercial UBD simulators. The Mukherjee and Brill correlation has been developed to overcome some of the limitations of the Beggs and Brill correlation (Brill & Mukherjee, 1999).

The Mukherjee and Brill correlation makes use of dimensionless gas and liquid velocity numbers and together with the inclination angle distinguishes between the different flow patterns. See Figure 8.

Table 1: Legend Figure 8

gv	= gas velocity
lv	= liquid velocity
sm	= transition slug to annular/mist
st	= stratified transition
bs	= bubble to slug transition

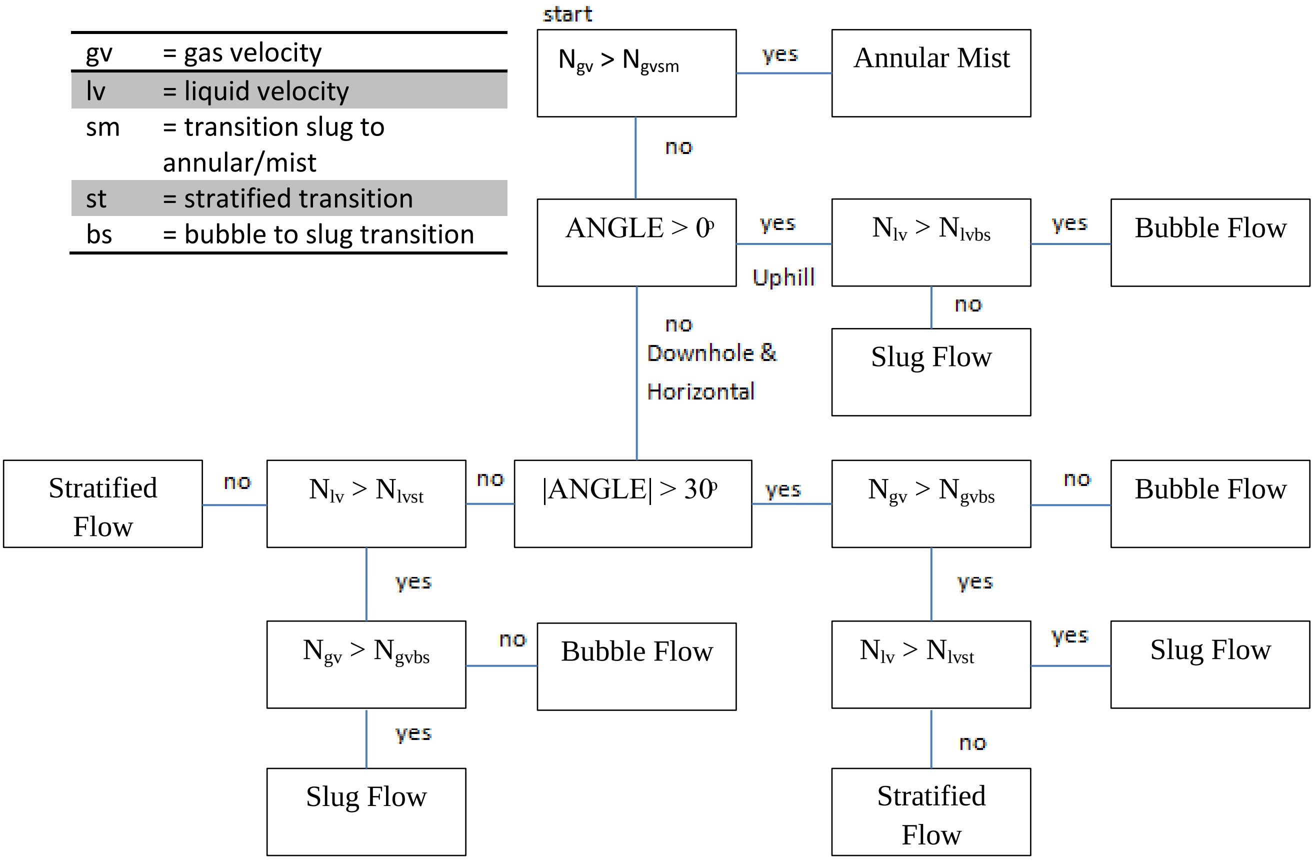

Figure 8: Flow chart to predict flow pattern transitions for the Mukherjee and Brill correlation

The friction factor in the Mukherjee and Brill correlation is obtained from the flow patterns with the aid of the Moody diagram. The Moody diagram is approximated by Colebrook and is based on the Reynolds number and annular roughness; see the appendix for the Matlab code. For annular flow a dimensionless friction ratio depending on liquid holdup is interpolated which is then multiplied by the Moody friction factor to get the right friction factor. For further details, see Brill & Mukherjee, (1999).

Developing an entire new model was beyond the scope of this project as well as implementing a commercial simulator into Matlab.

The basics of this Matlab code has therefore been obtained from the course AES1360 'Production Optimization' in the MSc. Petroleum Engineering & Geosciences at TU Delft.

The Matlab code works in the following way. In script 'Welloil_IL_vd_Sluijs' the input values are selected after which with the 'annuli' function file the script integrates back to the surface for each time step. For each integration step the 'Muk_Brill_dpds_an' function file calculates the different pressure drops utilizing all the other function files. In Figure 9 an overview of the modified code is presented.

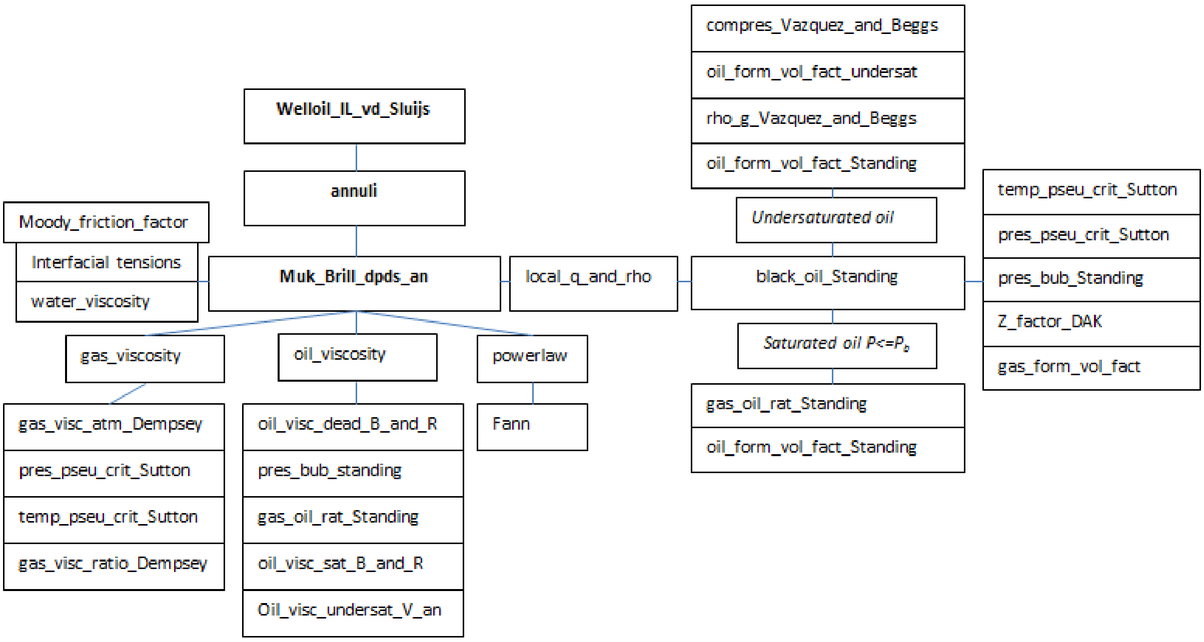

Figure 9: Overview of total Matlab code

2.3. Assumptions

Apart from the steady state assumption with which the Mukherjee and Brill created their empirical correlation, other assumptions are made to simplify the pressure drop calculation such as:

- No drill pipe rotation.
- Two-phase flow.
- Constant inflow of hydrocarbons and inflow at the bottom of the well.
- Constant annular geometry.
- No cuttings effect.
- While drilling ahead either vertically or deviated it is assumed that the BHP increases with the hydraulic gradient.
- Linear temperature profile.
- Mud column is defined by a power-law model.
- Eccentric annulus.
- Dry gas reservoir.
- Same rheological model for oil-base muds and water-base muds.

2.4. Modifications

Since the Mukherjee and Brill method originally was intended for pressure drop calculations in a production/injection wells, some modifications were required in order to use the model for pressure drop prediction in UBD.

- Diameter had to be adjusted to represent the hydraulic diameter. The hydraulic diameter refers to the diameter of the annulus between the casing and drill pipe or between an open hole section and drill pipe. The hydraulic diameter is defined by equation 2.4.1.

2.4.1 $dh = \frac{(dc^2 - dp^2)}{(dc + dp)}$ **(Jansen & Currie, 2010)**

- Surface area had to be adjusted so it represents annular casing/open hole-drill pipe geometry, see equation 2.4.2. [dc] represents the inner diameter of the hole being drilled and [dp] represents the outer diameter of the drill pipe.

2.4.2 $A = \frac{\pi(dc^2 - dp^2)}{4}$

- The effect of eccentricity is introduced into the model by replacing the friction factor equations with the power law model inside the following flow patterns: liquid flow, slug flow, bubble flow & annular flow. To be able to calculate the friction factor [f] the power law model utilizes the consistency index [K] and the flow behaviour index [n]. These are the parameters in equation 2.4.3 which relates shear stress [τ] to shear rate [γ]. See Figure 10 for the typical behaviour of a power-law fluid.

2.4.3 $\tau = K * \gamma^n$ **(ASME, 2005)**

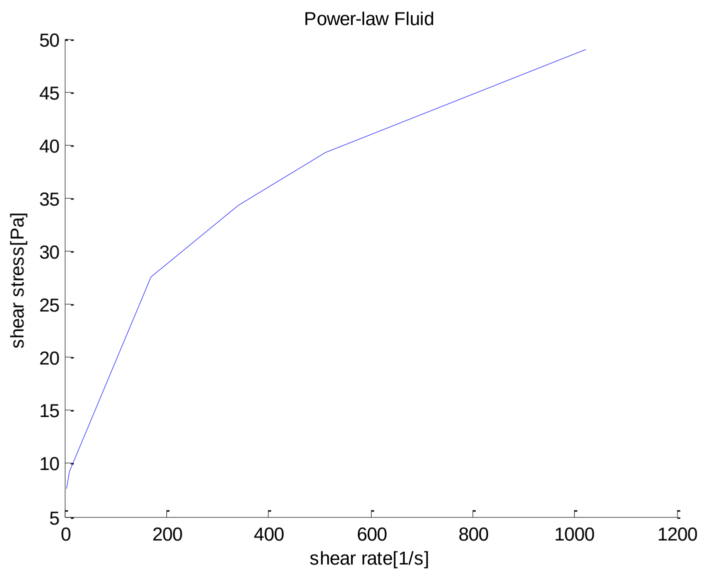

Figure 10: Typical behaviour of a power-law fluid

With the friction factor [f] calculated the concentric friction loss can be determined by equation 2.4.4.

2.4.4 $P_{fric} = \frac{-2*f*\rho*v^2}{dc-dp}$ **(Brill & Mukherjee, 1999)**

- Two empirical correlations based on the eccentricity factor[ec], flow behaviour index[n] and diameter ratio[k] have been found which calculate the correction factor. The correction factor needs to be multiplied with the concentric friction loss to find the eccentric friction loss: one correlation is valid for laminar flow and the other for turbulent flow, see respectively equation 2.4.5 and equation 2.4.6.

2.4.5 $R = 1 - \left(0.072 * \frac{ec}{n} * k^{0.8454}\right) - \left(1.5 * ec^2 * \sqrt{n} * k^{0.1852}\right) + \left(0.96 * ec^3 * \sqrt{n} * k^{0.2527}\right)$
(Haciislamoglu & Langlinais, 1990)

2.4.6 $R = 1 - \left(0.048 * \frac{ec}{n} * k^{0.8454}\right) - \left(0.67 * ec^2 * \sqrt{n} * k^{0.1852}\right) + \left(0.28 * ec^3 * \sqrt{n} * k^{0.2527}\right)$
(Aadnoy, Cooper, Miska, Mitchel, & Payne, 2009)

The effect of eccentricity on the correction factor determined by equations 2.4.5 and 2.4.6 can be seen in Figure 11. The explanation for the frictional pressure drop to be lower in an eccentric annuli can be seen in Figure 12.

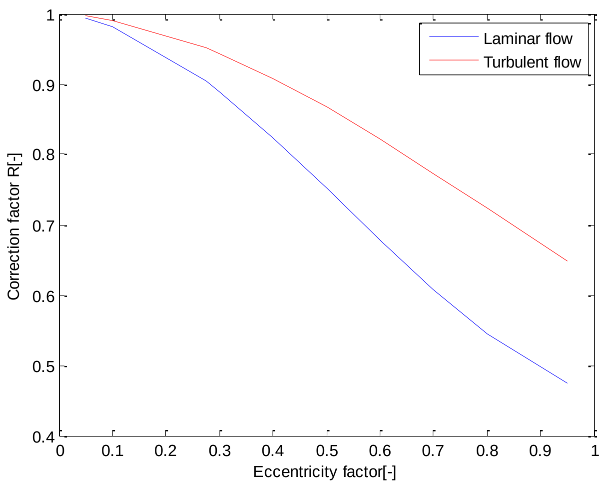

Figure 11: The effect of eccentricity on the correction factor

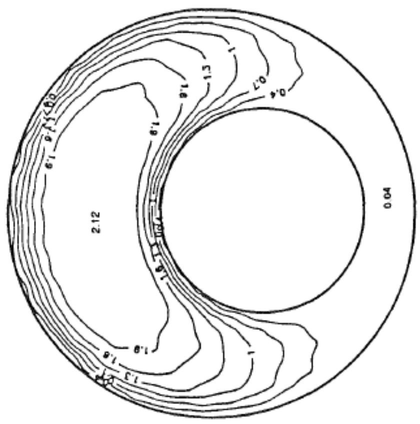

Figure 12: velocity profile of a yield-power law fluid eccentric annulus, ec = 0.5 (Haciislamoglu & Langlinais, 1990)

- To be able to predict the backpressure while drilling ahead an IF and FOR-loop combination which integrates back to surface for each time step is inserted. See Figure 13.

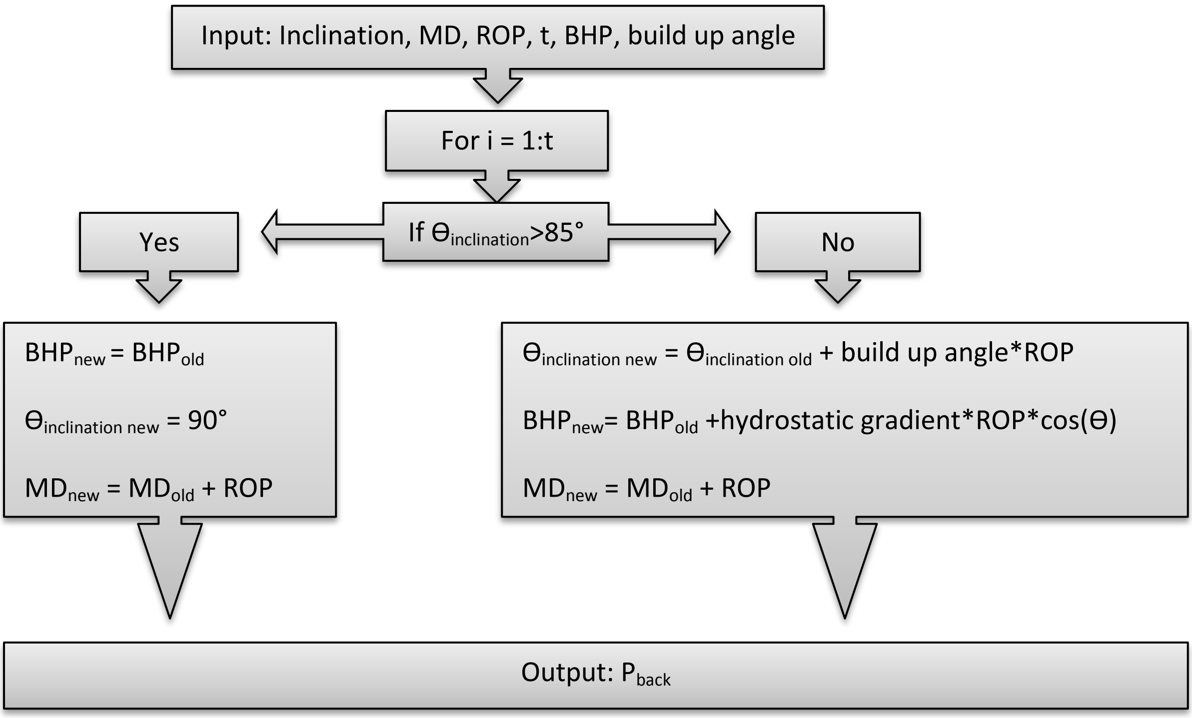

Figure 13: Block diagram of the loop calculating P_{back} for each time step

- To be able to plot Reynolds number, mixture/fluid velocity and type of flow regime along measured depth, this data is written to a document from which after each time step a figure is made.

3. Results

Table 2: Input values

Input values			
Fannreading	[16 21 65 85 100 135]	Ec	0.95 [-]
$\rho_{base\ oil\ mud}$	850 [kg/m^3]	Survey	Well CB21-2 China
$\rho_{base\ water\ mud}$	1000 [kg/m^3]	$d_{drill\ pipe}$	5 ½ [inch]
ρ_{gas}	0.95 [kg/m^3]	$d_{casing/open\ hole}$	8 ½ [inch]
ρ_{solid}	2500 [kg/m^3]	e	30e-6 [m]
GOR	2 [-]	T_tf	30 [°C]
q_{pump}	2000 [l/min]	T_wf	120 [°C]
t	60 [min]	ROP	50 [ft/hr]
P_wf	350 [bar]		

In Figure 14 the difference in each component of the total pressure drop between water-base mud and oil-base muds can be seen. Mainly the difference in p_{grav} due to density differences requires a higher P_{back} for OBM to achieve the same BHP.

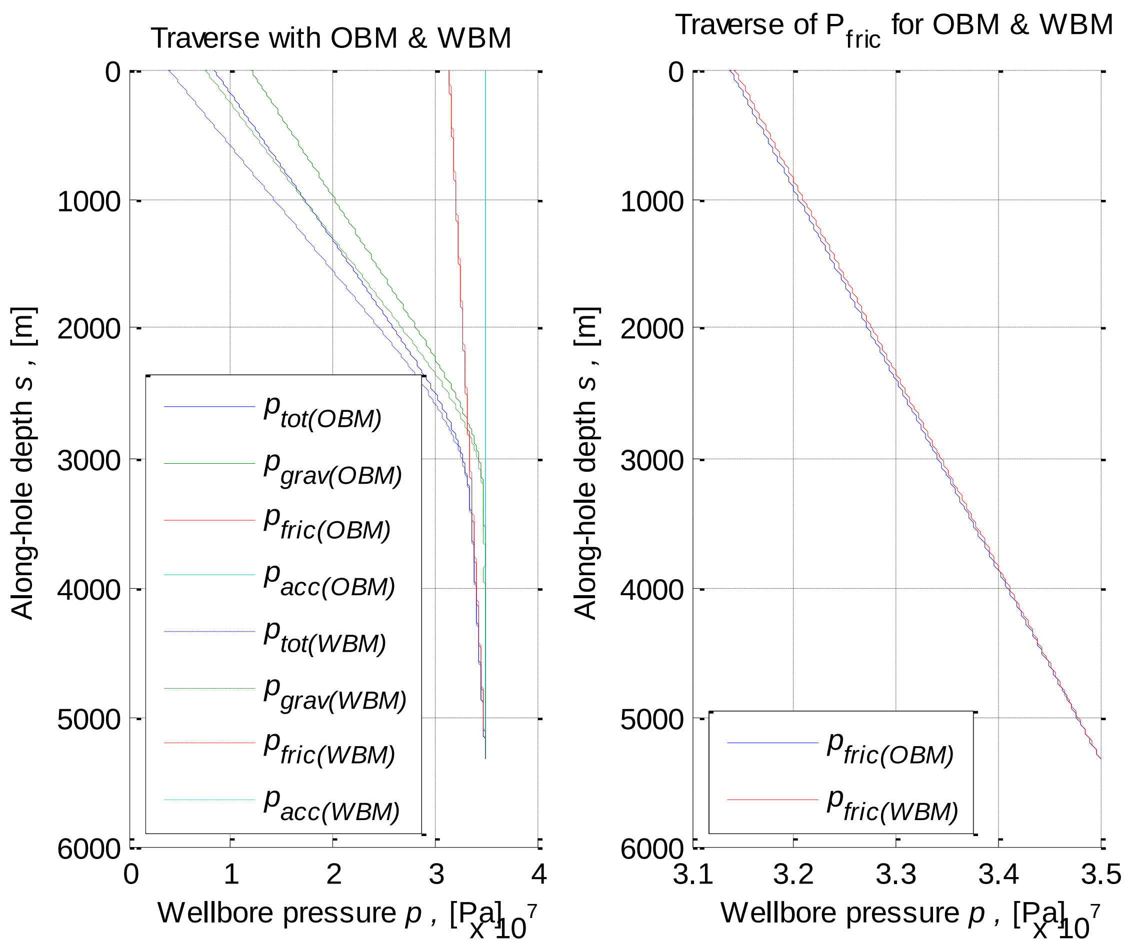

Figure 14: Traverse of well with BHP of 350 bar

In Figure 15 it can be seen that when drilling further horizontally for one hour (50ft) the frictional pressure drop increases were approximately 0.11 bar for OBM and 0.09 bar for WBM.

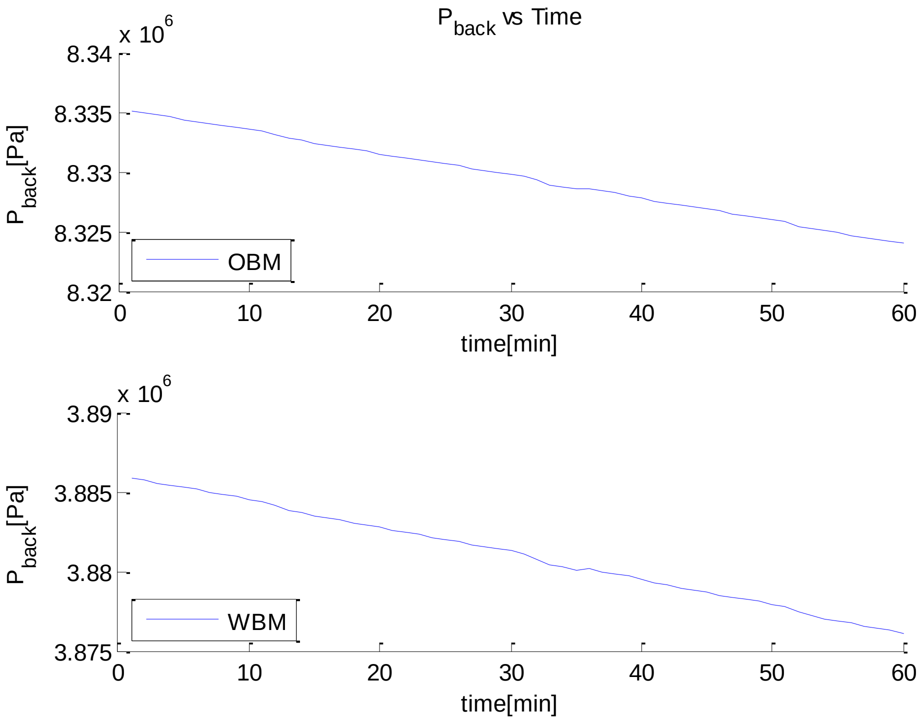

Figure 15: P_{back} vs. time

From Figure 16 the ability of oil to dissolve gas can clearly be seen. Flow regime '0' and '1' stand for liquid flow and bubble flow respectively.

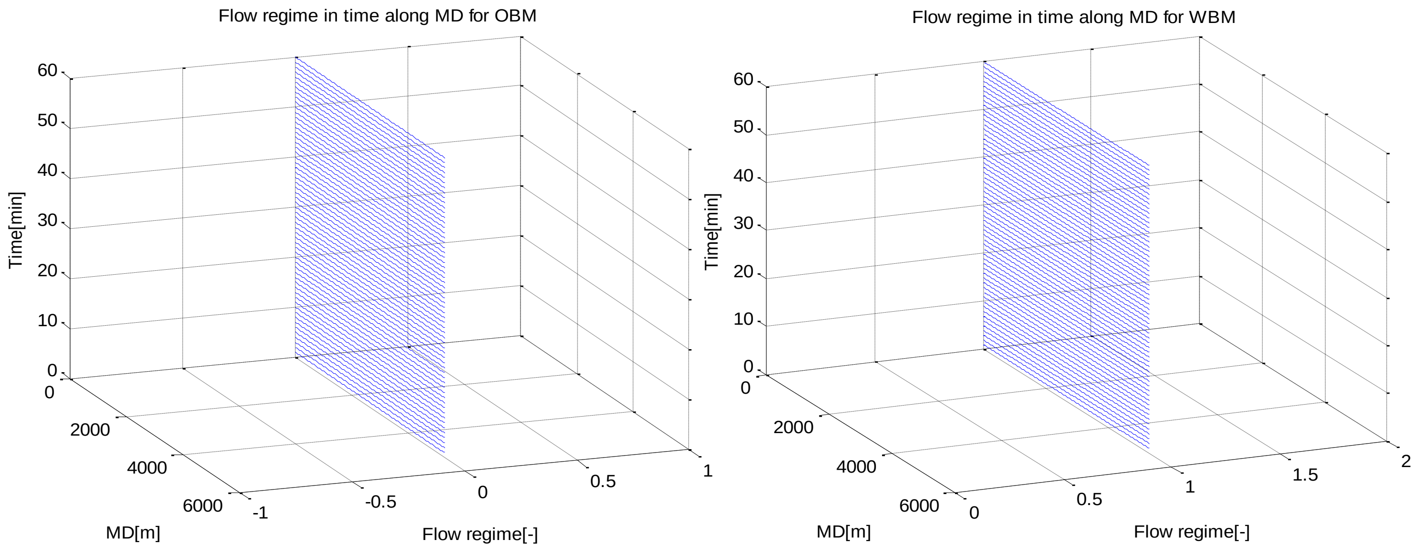

Figure 16: Flow regime for OBM and WBM

Figure 17 below shows that the Reynolds number for OBM decreases along the borehole due the decreasing fluid velocity along the borehole. For WBM this is the other way around due to the expansion of the gas close to the surface.

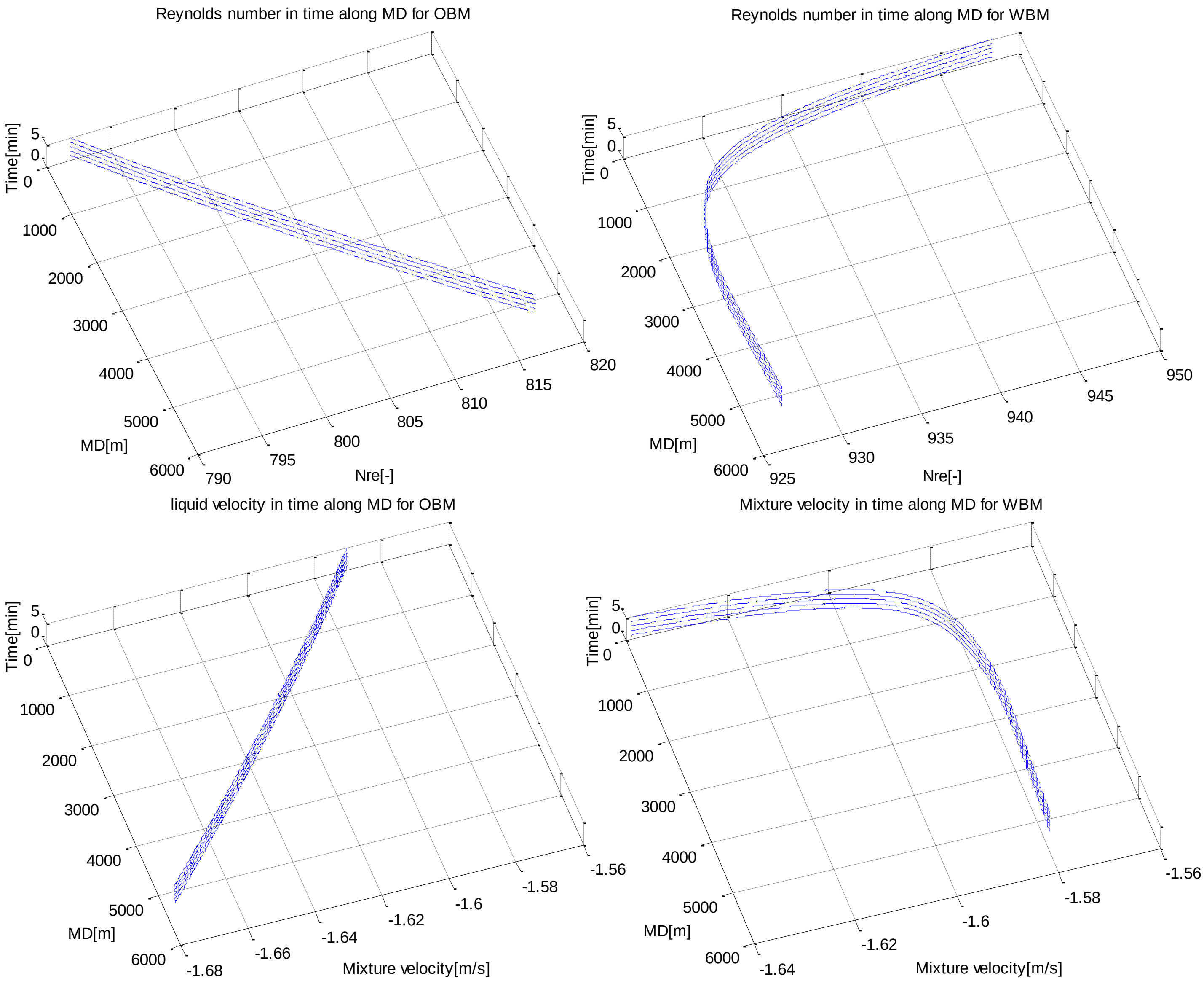

Figure 17: Reynolds number and fluid/mixture velocity along the borehole

See Figure 18 for the parameters which have the most effect on the frictional pressure drop, from high to low: Fluid behaviour index, Consistency index , Eccentricity factor. With the external factors its different for each type of mud for WBM it is pump rate and GOR and for OBM it is pump rate and BHT.

Table 3: input values, external sensitivity analysis

	Low		Average		High	
GOR	1	1.5	2	3	4	[-]
Pump rate	2000	2100	2200	2300	2400	[l/min]
BHT @ 3km	80	85	90	100	120	[°C]
ρ_{oil}	840	850	860	870	880	[kg/m^3]
ρ_{water}	1000	1025	1050	1100	1200	[kg/m^3]
ρ_{gas}	0.668	0.85	0.95	1.25	1.5	[kg/m^3]

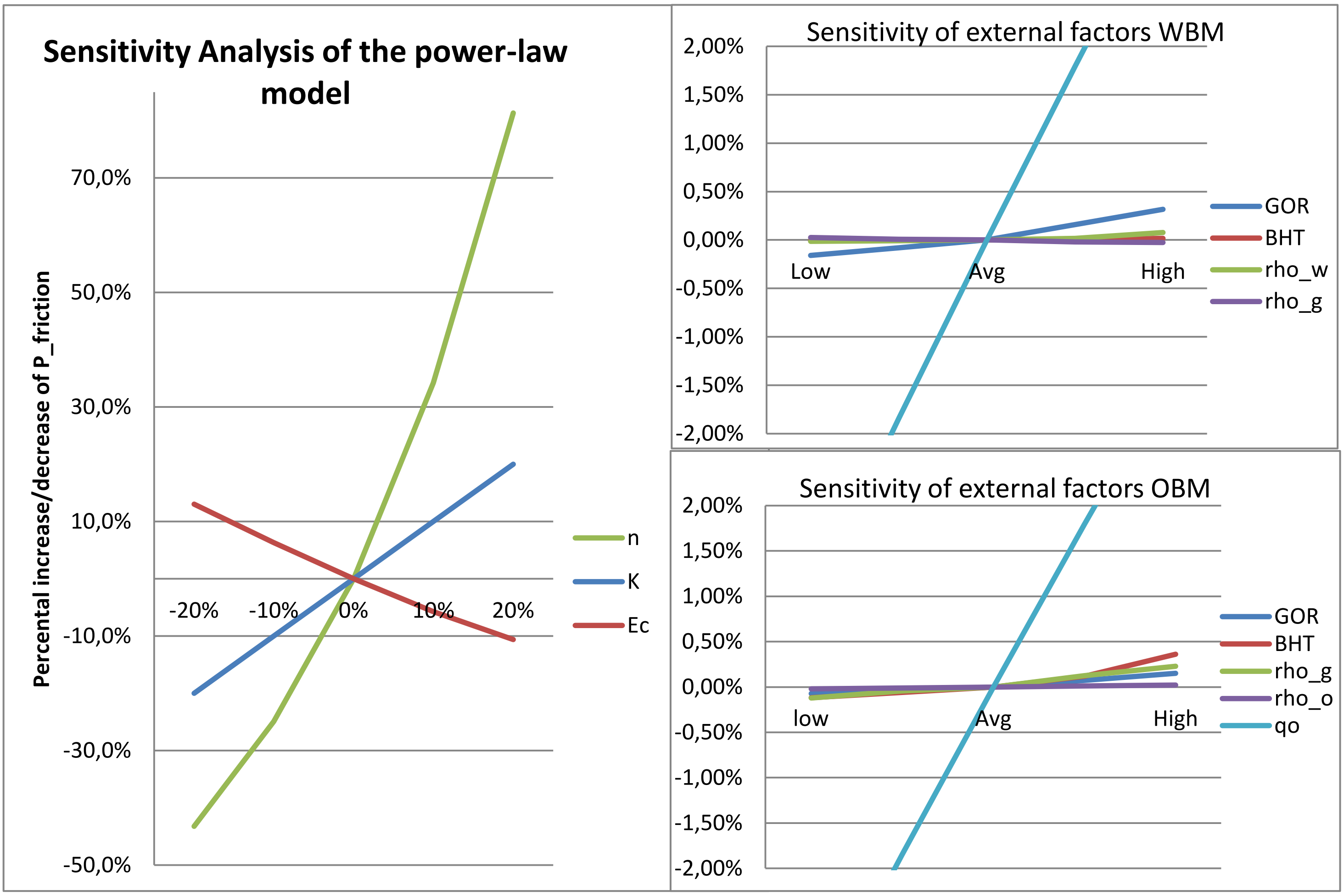

Figure 18: Sensitivity analysis

4. Discussion

Being able to simulate beforehand the different pressure drops that can be expected in the field has some major advantages: it allows for better selection of surface equipment, optimum mud properties, mitigating possible drilling problems and it makes it possible to drill underbalanced or with 'managed pressure'.

There are various models available based on either physical or empirical principles and the question still arises which one to use in a certain application? Hasan, Kabir, & Sayarpour, (2010) stated after statistical analysis of a couple different methods, that 'input data accuracy is the key to a model's performance.'

In this project the pressure drop in an underbalanced condition (inflow of dry reservoir gas) is simulated using Matlab. Although the program works and results can be obtained the question remains whether or not it gives a true estimation on the pressure drops experienced in the field. One way to criticize this program is by questioning the assumptions one by one.

Steady drill pipe: In case of coiled tubing drilling this is a reasonable assumption for rotary drilling however it depends on the hole & drill pipe size whether or not rotation has an effect on the frictional pressure loss. If we consider a 8 ½ inch hole with a 5 ½ inch drill pipe the annular high velocity flow path interacts with the viscous coupling thereby creating extra vortices/turbulence. This would increase the Reynolds number and thereby increases the annular frictional pressure drop. However if the hole is 9 7/8 inch or larger the viscous coupling only interacts with the 'dead' mud and therefore has a minimum effect on the annular frictional pressure drop. (Eck-Olsen, 2010) See Figure 19 for the effect of RPM and flow rate on the annular pressure drop for a tight annulus.

`

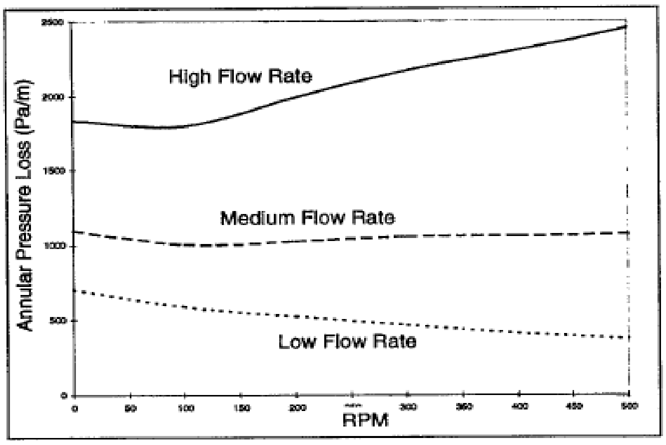

Figure 19: Annular pressure loss vs RPM for different flow rates (Rezmer-Cooper & Hutchinson, 1998)

Constant inflow of gas. This assumption is in practise invalid since while drilling ahead the contact area with the reservoir increases. Also the inflow of gas/oil/water occurs at different depths in the reservoir. Since underbalanced drilling takes place in geological basins which are completely understood, productive zones should be characterized and put into the model. When in practise additional gas/oil/water is encountered this model should be updated. This way the program knows what to expect and can therefore accurately predict the different pressure drops.

Constant annular geometry. In fact the drilling assembly varies in diameter with BHA and the tool joints having a bigger diameter than the drill pipe. Another possibility for a change in annular geometry along the well bore might be that a liner is installed instead of a casing. The tool joints can be neglected because of the small impact and the length of the joints. However the annular clearance near the BHA has a significant impact on the annular frictional pressure drop because of the rotational effects discussed above. Also the presence of a liner should definitely be included in the model.

No cuttings effect. In reality 2-6% of the cross-sectional area of an inclined well is occupied by cuttings. A rough estimation therefore is that 97% of the cuttings get suspended in the mud (Skalle, 2009). At a flow rate of 2000l/min it represents approx. 0.4% of the volume that gets circulated, something we can neglect. But it is the 3% of the cuttings which don't get suspended which causes solids build up in certain parts of the well thereby creating an alternating process of normal speed flow(clear annulus) and high speed flow(small annular clearance). In ERD wells a so called extra 'junk slot' is drilled to avoid any stuck pipe because you can't clean the hole for 100% (Eck-Olsen, 2010). See Figure 20 for the effect of cuttings on the ECD as function of flow.

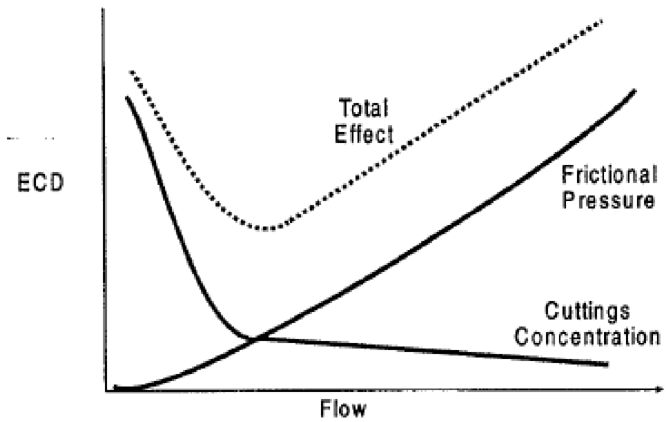

Figure 20: Cuttings loading vs. Flow (Rezmer-Cooper & Hutchinson, 1998)

A power-law model. To properly evaluate the wellbore hydraulics a rheological model is required which accurately describes the relation between shear rate and shear stress. There are four main different rheological models: Newtonian, Bingham plastic, Power-law and the Herschel-Bulkley model. Since most drilling muds are non-Newtonian fluid with shear stress decreasing as shear rate increases, this behaviour is best described by either the Power-law or the Herschel-Bulkley model. Between these two models it is the Herschel-Bulkley model aka yield power-law which describes the majority of the drilling fluids the most accurate. No research has been published to develop a correlation which includes eccentricity in frictional pressure loss calculations for the Herschel-Bulkley model, therefore the power-law model is utilized in this software tool.

When drilling ahead either vertically or deviated the BHP increases with hydrostatic pressure. In practice this is a reasonable assumption although if HTHP formations are encountered it is disputable.

Linear temperature profile. Temperature is an important parameter in defining the formation volume factors especially that of oil. It depends on the location of the rig and the geological setting whether or not this is a valid assumption. For example in the case of offshore wells and HTHP formations a linear temperature profile might be a wrong assumption. Since this well is drilled onshore the linear temperature profile is a valid assumption.

Last but not least the identical rheological model for both OBM as WBM. This assumption is invalid if the shear rate-shear stress relation is not identical. The input of the correct rheological model and the accurate parameters is very important because of the great impact on the frictional pressure drop, see Figure 18.

Looking at the results for OBM and WBM, it can be concluded that with the given input parameters there isn't much difference in frictional pressure loss between the two base muds, the main reason being the identical rheological model. For this particular example it depends on the limit of the backpressure that can be applied by the choke and the desired BHP which of the two muds to use. It might be an idea to use OBM for gas reservoirs due to its ability to dissolve gas and the little sensitivity towards an unexpected inflow of extra hydrocarbon gas, see Figure 18.

5. Conclusions

Based on the works of this project, the following conclusions and recommendations can be made:

- Using the Mukherjee and Brill method in Matlab to predict the pressure drops in an underbalanced well operation is possible, however these predictions require validation.

- Although the model works, it is recommend that more research should be put into an empirical/physical principle that combines drill pipe rotation, eccentricity and the effect of cuttings as these factors have a major impact on the frictional pressure drop.

- For the assumptions: constant inflow of gas, inflow at the bottom of the well, hydraulic gradient, linear temperature profile and annular geometry. The best and ideal case would be if annular geometry, temperature and pore pressure are assigned to each of formations within the geological setting and this geological model is used by the drilling simulator. So when the simulator integrates back to the surface or to the bottom it uses the formation parameters corresponding to that TVD.

- When drilling underbalanced it is extremely important to accurately predict the frictional pressure drop just outside or inside the reservoir. This is due to one major reason, the chance of rapid impairment of the reservoir due to a sudden overbalanced condition.

- The most important factor affecting the frictional pressure drop is the rheological model being used. Therefore selecting the model which fits the shear rate-shear stress behaviour best is of great importance.

Nomenclature

BHA	= Bottom hole Assembly
BHP	= Bottom hole pressure
BHT	= Bottom hole Temperature
BOP	= Blowout preventer
ECD	= Equivalent circulating density
ERD	= Extended reach drilling
ESD	= Electronic shut-in device
GOR	= Gas to oil ratio
HTHP	= High Pressure High Temperature
MD	= Measured Depth
MPD	= Managed pressure Drilling
OBM	= Oil-base mud
PWD	= Pressure while Drilling
RCH	= Rotating Control Head
RF	= Recovery Factor
ROP	= Rate of Penetration
TVD	= True Vertical Depth
UBD	= Underbalanced Drilling
WBM	= Water-base mud

A	= Annular area
dc	= Inner diameter casing/open hole
dh	= Hydraulic diameter
dp	= Outer diameter drill pipe
ec	= Eccentricity factor
f	= Friction factor
K	= Consistency index
n	= Flow behaviour index
N_{gv}	= Dim. gas velocity
N_{gvbs}	= Dim. gas velocity transition between bubble and slug flow
N_{gvsm}	= Dim. Gas velocity transition between slug and annular/ mist flow
N_{lv}	= Dimensionless liquid velocity
N_{lvbs}	= Dim. gas velocity transition between bubble and slug flow
N_{lvst}	= Dim. gas velocity transition to stratified flow
Nre	= Reynolds number
R	= Correction factor
t	= Time
T	= Temperature
v	= Velocity
γ	= Shear rate
Θ	= Angle
ρ	= Density
τ	= Shear stress

References

Aadnoy, B., Cooper, I., Miska, S., Mitchel, R., & Payne, M. (2009). *Advanced Drilling and Well Technology.* Richardson, Texas, USA: Society of Petroleum Engineers.

Airdrilling. (2005). Retrieved April 4, 2011, from Airdrilling: http://www.airdrilling.com/applications/underbalanced-drilling

ASME. (2005). *Drilling Fluids Processing handbook.* Burlington, USA: Elsevier.

Bennion, D., Thomas, F., Bietz, R., & Bennion, D. (2002). Underbalanced Drilling. *SPE reprint series no. 54*, 17-25.

Brill, P., & Mukherjee, H. (1999). *Multiphase Flow in Wells.* Richardson, Texas, USA, Texas, United States of America: SPE.

Eck-Olsen, M. (2003). *IADC Rigpass.* Bergen, Norway: Statoil.

Eck-Olsen, M. (2010). TPG 4215: High Deviation Drilling. Trondheim, Norway: NTNU.

Haciislamoglu, M., & Langlinais, J. (1990). Non-Newtonian flow in eccentric annuli. *ASME, Journal of Energy Recources Technology vol. 112*, 163-169.

Hasan, A., Kabir, C., & Sayarpour, M. (2010, February 16). simplified two-phase flow modeling in wellbores. *Journal of Petroleum Science and Engineering no. 72*, pp. 42-49.

IHRDC. (n.d.). Retrieved February 4, 2011, from PASCO: http://copas-pasco.com/uploads/9._UNDERBALANCED_DRILLING_101.pdf

Institution, T. P. (n.d.). Retrieved February 5, 2011, from http://www.priweb.org: http://www.priweb.org/ed/pgws/history/spindletop/spindletop.html

Jansen, J., & Currie, P. (2010). *Modelling and optimisation of oil and gas production systems.* Delft: TU Delft.

Lage, A., Fjelde, K., & Time, R. (2000). Underbalanced Drilling Dynamics: Two-Phase Flow Modeling and Experiments. *IADC/SPE 62743.* Kuala Lumpur, Malaysia, 11-13 September: IADC/SPE Asian Pacific Drilling Technology Conference.

Pérez-Téllez, C., Smith, J., & Edwards, J. (2002). A new comprehensive, mechanistic model for underbalanced drilling improves wellbore pressure predictions. *SPE 74426.* Villahermosa, Mexico: SPE International Petroleum Conference and Exhibition, 10-12 February.

Qutob, H. (2007-2008). Retrieved February 4, 2011, from queensland.spe.org: http://queensland.spe.org

Rezmer-Cooper, & Hutchinson. (1998). Using downhole annular pressure measurements to anticipate drilling problems. *SPE 49114.* New Orleans, Louisiana: SPE Annual Technical Conference and Exhibition, 27-30 September.

Saponja, J. (2002). Underbalanced Drilling. *SPE Reprint Series no. 54*, 9-16.

Skalle, P. (2009). *Drilling Fluid Engineering.* Trondheim: NTNU.

Appendices

Head script:

```
%% Script to compute the pressure drop over an inclined well.

% Reference:
% [1] AES1360 Production Optimisation TU Delft

clear all
close all
clc
% delete 'flow_reg.txt' 'Nre_ec.txt' 'Nre.txt' 'mixture_velocity'
% ----------------------------------------------------------------------------
% Input data:
% ----------------------------------------------------------------------------
% Mud properties to determine K and n powerlaw fluid should be a vector
Fannreading=[16 21 65 85 100 140];
% Eccentricty of well
ec= 0.75; % Eccentricity ratio
% Survey input
importfile('Survey.xlsx'); % Survey of well trajectory
Inclination = from_deg_to_rad(Inclination);
alpha=[MD Inclination];
% Annular geometry
dp = from_in_to_m(5.5); % drill pipe outside diameter, m
dc = from_in_to_m(8.5); % diameter hole being drilled, m

% Multi-phase gas-oil-water flow, using the Mukherjee and Brill correlation
% Rates at surface
GOR = 2; % Producing ratio of gas over oil
%% OBM
q_o_sc = from_lpm_to_m3_per_s(-2200); % oil rate  at st. cond., m^3/s.
q_g_sc = q_o_sc*GOR; % gas rate at st. cond., m^3/s.
q_w_sc = 0; % water rate  at st. cond., m^3/s.
%% WBM
% q_o_sc = 0;
% q_w_sc = from_lpm_to_m3_per_s(-2000);
% q_g_sc = q_w_sc*GOR;
%% General info
% Note: flow rates should have positive values for a production well.
rho_s_sc = 2500; % solid density at st. cond., kg/m^3.
rho_g_sc = 0.95; % gas density at st. cond., kg/m^3.
rho_o_sc = 860;  % oil density at st. cond., kg/m^3.
rho_w_sc = 1050; % water density at st. cond., kg/m^3.
e = 30e-6; % annulur rougness, m
s_tot = alpha(end,1); % total along-hole well depth from survey, m
T_tf = 30; % tubing head temperature, deg. C
T_wf = 90; % bottomhole temperature, deg. C
% Create data vectors:
q_sc = [q_g_sc,q_o_sc,q_w_sc];
rho_sc = [rho_g_sc,rho_o_sc,rho_w_sc];
% Compute the FBHP by integrating from 0 to s_tot
p_wf =
annuli(alpha,dp,dc,e,p_tf,q_sc,rho_sc,0,s_tot,T_tf,T_wf,Fannreading,ec);
```

```
%% Extra information for the drilling simulator
ROP = from_ft_to_m(50)/60; % Rate of Penetration, m/min
t = 5; % Drilling time, min
p_tf = 50e5; % FTHP(backpressure), Pa.
%% UBD Simulator

for i=1:t
if alpha(end,2)>=1.5 %horizontal drilling p_wf should be constant
        Inclination(end+1)=from_deg_to_rad(90);
        s_tot=alpha(end+1-i,1)+ROP;
        MD(end+1)=s_tot;
        alpha=[MD Inclination];
        p_tf(i) =
annuli(alpha,dp,dc,e,p_wf,q_sc,rho_sc,s_tot,0,T_wf,T_tf,Fannreading,ec);
        % for profiles like: flow_regime, mixture_velocity, Reynolds number
%         fid = fopen('Nre.txt'); %flow_reg = fread(fid);
%         Reynolds_nr = str2num(fscanf(fid,'%c'));
%         fclose(fid);
%         delete 'Nre.txt'
%         s = 0:s_tot/(length(Reynolds_nr)-1):s_tot;
%         s = fliplr(s);
%         time = ones(length(Reynolds_nr),1).*i;
%         plot3(s,Reynolds_nr,time);
%         title('Reynolds number in time along MD for WBM');
%         xlabel('MD[m]');ylabel('Nre[-]');zlabel('Time[min]');
%         hold on;

else % For vertical or deviated drilling p_wf shouldn't be constant but
increase with approx. hydrostatic gradient
    Inclination(end+1)=Inclination(end)+from_deg_to_rad(5)*ROP;
    s_tot=alpha(end,1)+ROP;
    MD(end+1)=s_tot;
    alpha=[MD Inclination];
% Letting p_wf increase with hydrostatic gradient 1bar per 10m
    p_wf=p_wf+cos(Inclination(end))*(MD(end)-MD(end-1))*1e4;
    p_tf(i) =
annuli(alpha,dp,dc,e,p_wf,q_sc,rho_sc,s_tot,0,T_wf,T_tf,Fannreading,ec);
end
end
t=1:t;
% hold off; figure
plot(t,p_tf);
xlabel('time\it t,\rm min');
ylabel('Backpressure\it Pback,\rm Pa');
grid on
%% Plotting the traverse
[p_tf,s,p] =
annuli(alpha,dp,dc,e,p_wf,q_sc,rho_sc,s_tot,0,T_wf,T_tf,Fannreading,ec);
figure
plot(p,s)
axis ij
xlabel('Wellbore pressure\it p ,\rm Pa')
ylabel('Along-hole depth\it s ,\rm m')
grid on
legend('\itp_{tot}','\itp_{grav}','\itp_{fric}','\itp_{acc}',3)
%% Influence of cuttings on the density of the mud
[Vt,percentage_solid] =
per_solid_in_mudvolume(q_sc,p_wf,T_wf,dc,ROP,rho_sc);
disp('Percentage of cuttings in the mud');disp(percentage_solid);
% The effect of cuttings on the total density of the mud can be neglected
```

Integrating script:

```
function [p_out,s,p] = annuli(alpha,dp,dc,e,p_in,q_sc,rho_sc,s_in,s_out,
...T_in,T_out,Fannreading,ec)
% [p_out,s,p] = pipe(alpha,dpipe,dbit,e,fluid,p_in,q_sc,rho_sc,s_in,s_out,
...T_in,T_out)
%
% Computes the pressure p_out at along-hole distance s_out in a deviated
% pipe element for a given pressure p_in at along-hole distance p_in,
% through numerical integration from s_in to s_out.
% alpha = inclination wrt. vertical, rad; alternatively alpha can be a
%    survey file (matrix) with AHD values in the first column (in m) and
%    inclination values in the second column (in rad).
% dp = outside diameter drill pipe, m
% dc= diameter hole being drilled, m
% e = roughness, m
% p = [p_tot,p_grav,p_fric,p_acc], Pa
%   p_acc  = p_in + pressure increase due to acceleration losses, Pa
%   p_fric = p_in + pressure increase due to friction losses, Pa
%   p_grav = p_in + pressure increase due to head loss, Pa
%   p_tot  = p_in + pressure increase due to gravity, friction and
%            acceleration losses, Pa
% p_in = pressure at s_in, Pa
% p_out = pressure at s_out, Pa
% q_sc = [q_g_sc,q_o_sc,q_w_sc], m^3/s
%   q_g_sc = gas flow rate at st. cond., m^3/s.
%   q_o_sc = oil flow rate at st. cond., m^3/s.
%   q_w_sc = water flow rate at st. cond., m^3/s.
%   Note: Flowrates in a production well need to have a negative value.
% rho_sc = [rho_g_sc,rho_o_sc,rho_w_sc], kg/m^3
%   rho_g_sc = gas density at st. cond., kg/m^3.
%   rho_o_sc = oil density at st. cond., kg/m^3.
%   rho_w_sc = water density at st. cond., kg/m^3.
% s = co-ordinate running from the separator to the reservoir, m
% s_in = starting point for the integration
% s_out = end point for the integration
% T_in = temperature at s_in, deg. C
% T_out = temperature at s_out, deg. C

% Reference: AES1360 Production Optimisation TU Delft

interval = [s_in,s_out]; % integration interval, m
boundcon = [p_in,p_in,p_in,p_in]; % boundary condition, Pa
%% options = []; % dummy variable, -
options = odeset('MaxStep',10,'RelTol',1e-3);
% Tight tolerances to obtain better quality plots. Time consuming!
%% multi-phase, Mukherjee & Brill
[s,p] = ode45('Muk_Brill_dpds_an',interval,boundcon,options,alpha,dp,dc,e,
...q_sc,rho_sc,s_in,s_out,T_in,T_out,Fannreading,ec);
n = length(p);
p_out = p(n,1);
```

Mukherjee & Brill correlation:

```
function dpds = Muk_Brill_dpds_an(s,p,flag,alpha,dp,dc,e,q_sc,rho_sc,s_in,
...
                                s_out,T_in,T_out,Fannreading,ec)
% dpds = Muk_Brill_dpds(s,p,flag,alpha,d,e,q_sc,rho_sc,s_in, ...
%                        s_out,T_in,T_out)
%
% Computes the derivative dp/ds for a given pressure p and along-hole
% distance s, in an element of a flowline-wellbore system. The distance s
% is measured from the separator towards the reservoir. Therefore,
% flowrates are negative for production wells.
%
% Uses the Mukherjee and Brill correlation for multiphase flow in inclined
% wells; see references [1] and [2]. A reality check has been added to
% ensure that the computed liquid hold-up (for flow with slip) is never
% smaller than the in-situ liquid volume fraction (the 'no-slip hold-up').
%
% The vector p contains the total pressure, and the pressures taking into
% account the individual effects of gravity, friction and acceleration
losses
% respectively. Accordingly, the vector dpds contains the total pressure
loss
% per unit length, as well as the individual gravity losses, friction
% losses and acceleration losses.
%
% This function can be used to compute the pressure drop through numerical
% integration. It has the correct format to be used in conjunction with one
of
% the standard numerical integration routines in MATLAB.
%
% alpha = inclination wrt. vertical, rad; alternatively alpha can be a
%    survey file (matrix) with AHD values in the first column (in m) and
%    inclination values in the second column (in rad).
% dpipe = outside diameter of drill pipe, m
% dbit= outside diameter of bit, m
% dpds = [dpds_tot;dpds_grav;dpds_fric;dpds_acc]
% dpds_acc  =  pressure gradient due to acceleration losses, Pa/m
% dpds_fric =  pressure gradient due to friction losses, Pa/m
% dpds_grav = pressure gradient due to head losses, Pa/m
% dpds_tot  = dpds_grav + dpds_fric + dpds_acc = total pressure gradient,
Pa/m
% e = roughness, m
% flag = dummy variable, -
% p = [p_tot,p_grav,p_fric,p_acc], Pa
% p_acc  = p_in + pressure increase (decrease for production wells) due to
%          acceleration losses, Pa
% p_fric = p_in + pressure increase (decrease for production wells) due to
%          friction losses, Pa
% p_grav = p_in + pressure increase (decrease for production wells) due to
%          head loss, Pa
% p_tot  = p_in + pressure increase (decrease for production wells) due to
%          gravity, friction and acceleration losses, Pa
% p_in = pressure at s_in, Pa
% p_out = pressure at s_out, Pa
% q_sc = [q_g_sc,q_o_sc,q_w_sc], m^3/s
% q_g_sc = gas flow rate at standard conditions, m^3/s
% q_o_sc = oil flow rate at standard conditions, m^3/s
% q_w_sc = water flow rate at standard conditions, m^3/s
% rho_sc = [rho_g_sc,rho_o_sc,rho_w_sc], kg/m^3
% rho_g_sc = gas density at standard conditions, kg/m^3
% rho_o_sc = oil density at standard conditions, kg/m^3
```

```
% rho_w_sc = water density at standard conditions, kg/m^3
% s = along-hole distance, measured from the separator to the reservoir, m
% s_in = starting point for the integration
% s_out = end point for the integration
% T_in = temperature at s_in, deg. C
% T_out = temperature at s_out, deg. C

% References:
% [1] Mukherjee,H. and Brill, J.P., 1985: Pressure drop correlations for
% inclined two-phase flow, J. Energy Resources Techn., vol. 107, p.549.
% [2] Brill, J.P. and Mukherjee, H., 1999: Multiphase flow in wells, SPE
% Monograph Series, vol 17., SPE, Richardson.
% [3] AES1360 Production Optimisation TU Delft

% Check sign of pressure:
p_tot = p(1); % first element of vector p is the total wellbore pressure,
Pa
if p_tot < 0
    warning('Negative pressure.')
end

% Determine inclination in case of survey file input:
if length(alpha) > 1
    n_sur = length(alpha(:,1)); % number of survey points
    if s < alpha(1,1)
        help = alpha(1,2);
    else if s > alpha(n_sur,1)
        help = alpha(n_sur,2);
        else
            help = interp1(alpha(:,1),alpha(:,2),s);
        end
    end
    clear alpha;
    alpha = help; % replace survey file by single inclination value, rad
end

% Compute internal variables:
dh=(dc^2-dp^2)/(dc-dp); % hydraulic diameter
A = (pi*(dc^2-dp^2))/4;% cross-sectional area of the annulus, m^2
epsilon = e/dh; % dimensionless pipe roughness, -
g = 9.81; % acceleration of gravity, m/s^2

% Compute temperature through linear interpolation between T_in and T_out:
T = T_in+(T_out-T_in)*(s-s_in)/(s_out-s_in); % temperature, deg. C
T_abs = T + 273.15; % absolute temperature, K

% Densities and flow rates at standard conditions:
rho_g_sc = rho_sc(1); % gas density at standard conditions, kg/m^3
rho_o_sc = rho_sc(2); % oil density at standard conditions, kg/m^3
q_g_sc = q_sc(1); % gas flow rate at standard conditions, m^3/s
q_o_sc = q_sc(2); % oil flow rate at standard conditions, m^3/s

% Compute local gas and liquid properties:
R_go = q_g_sc/q_o_sc; % producing GOR as would be observed at surface,
m^3/m^3
R_sb = R_go; % This is the bubble point GOR for the oil in the wellbore.
This value may be much higher than R_sb in the reservoir if gas-cap gas
             % or lift gas is produced.
```

```
[q,rho] = local_q_and_rho(p_tot,q_sc,R_sb,rho_sc,T);
% q = [q_g, q_o, q_w], m^3/s, rho = [rho_g, rho_o, rho_w], kg/m^3
q_g = q(1); % local gas flow rate, m^3/s
q_o = q(2); % local oil flow rate, m^3/s
q_w = q(3); % local water flow rate, m^3/s

rho_g = rho(1); % local gas density, kg/m^3
rho_o = rho(2); % local oil density, kg/m^3
rho_w = rho(3); % local water density, kg/m^3

mu_g = gas_viscosity(p_tot,rho_g_sc,T); % local gas viscosity, Pa s
mu_o = oil_viscosity(p_tot,R_sb,rho_g_sc,rho_o_sc,T); % local oil
viscosity, Pa s
mu_w = water_viscosity; % input function; local water viscosity, Pa s

sigma = interfacial_tensions; % input function; sigma = [sigma_go,
sigma_gw];
sigma_go = sigma(1); % gas-oil interfacial tension, N/m
sigma_gw = sigma(2); % gas-water interfacial tension, N/m

f_o = q_o/(q_o+q_w); % local oil fraction , -
f_w = q_w/(q_o+q_w); % local water fraction, -

q_l = q_o + q_w; % local liquid flow rate, m^3/s
rho_l = rho_o*f_o + rho_w*f_w; % local liquid density, kg/m^3
mu_l = mu_o*f_o + mu_w*f_w; % local liquid viscosity, Pa s
sigma_gl = sigma_go*f_o + sigma_gw*f_w; % local gas-liquid interf. tension,
N/m

% Compute superficial and mixture velocities:
v_sg = q_g/A; % local superficial gas velocity, m/s
v_sl = q_l/A; % local superficial liquid velocity, m/s
v_m = v_sg + v_sl; % local mixture velocity, m/s

% Check for free gas:
if abs(q_g) < 1e-12 % no free gas - liquid flow only
    flow_reg = 0; % liquid-only flow
%     V_sl = num2str(v_sl);
%     fid = fopen('mixture_velocity.txt','a');
%     fprintf(fid,'\t%s',V_sl);
%     fclose(fid);
%     fid = fopen('flow_reg.txt','a');
%     fwrite(fid,flow_reg);
%     fclose(fid);
%     Compute pressure gradient for liquid-only flow:
    v_m = v_sl; % local liquid velocity, m/s
    rho_n = rho_l; % local liquid density
    dpds_grav = rho_l*g*cos(alpha); % gravity losses, Pa/m
    f_r = 1; % linear interpolation of friction factor ratio(slip,no-slip)
    % Eccentric friction loss power-law fluid Pa/m
    dpds_fric = powerlaw(v_m,f_r,rho_n,1,dp,dc,Fannreading,ec,flow_reg);
    dpds_acc = 0; % acceleration losses are neglegible, Pa/m
    dpds_tot = dpds_grav + dpds_fric + dpds_acc; % total pressure grad.,
Pa/m
    dpds = [dpds_tot;dpds_grav;dpds_fric;dpds_acc];
else % gas-liquid flow

    % Determine flow direction (uphill, downhill or horizontal)
    if v_m > 0 % flow from wellhead to bottomhole (injection well)
```

```
        if  alpha < pi/2 % 'downhill' drilled well section (usual
situation)
            flow_dir = -1; % downhill flow
        else
            if  alpha > pi/2 % 'uphill' drilled well section (occurs
                             % occasionally in 'horizontal' wells)
                flow_dir = 1; % uphill flow
            else % alpha = pi/2, horizontal well section
                flow_dir = 0; % horizontal flow
            end
        end
    else % flow from bottomhole to wellhead (production well)
        if  alpha < pi/2 % 'downhill' drilled well section
            flow_dir = 1; % uphill flow
        else
            if alpha > pi/2 % 'uphill' drilled well section
                flow_dir = -1; % downhill flow
            else % alpha = pi/2, horizontal well section
                flow_dir = 0; % horizontal flow
            end
        end
    end

    % Determine the value of theta_MB. This is the angle as defined in the
    % original publication of Mukherjee and Brill.
    theta_MB = flow_dir*abs(alpha-pi/2); % theta_MB is negative for
downward
                                          % and positive for upward flow

    % Compute Duns and Ros' dimensionless numbers:
    N_lv = abs(v_sl)*(rho_l/(g*sigma_gl))^(1/4); % liquid velocity number,
-
    N_gv = abs(v_sg)*(rho_l/(g*sigma_gl))^(1/4); % gas velocity number, -
    N_l = mu_l*(g/(rho_l*sigma_gl^3))^(1/4); % liquid viscosity number, -

    % Determine flow pattern boundaries:
    help01 = sin(theta_MB);

    help02 = (log10(N_gv) + 0.940 + 0.074*help01 - 0.855*help01^2 +
3.695*N_l);
    N_lv_bs = 10^help02; % upflow bubble-slug transition boundary, -

    help03 = 1.401 - 2.694*N_l + 0.521*N_lv^0.329;
    N_gv_sm = 10^help03; % universal slug-mist transition boundary, -

    help04 = log10(N_lv);
    help05 = 0.431 - 3.003*N_l - (1.138*help04 + 0.429*help04^2 - 1.132) *
...
             help01;
    N_gv_bs = 10^help05; % downflow and horizontal bubble-slug transition
                         % boundary, -

    help06 = log10(N_gv);
    help07 = 0.321 - 0.017*N_gv - 4.267*help01 - 2.972*N_l - ...
             0.033*help06^2 - 3.925* help01^2;
    N_lv_st = 10^help07; % downflow and horizontal stratified flow
boundary, -
```

```
% Determine flow pattern:
    if N_gv >= N_gv_sm
        flow_reg = 3; % annular mist flow
    else
        if theta_MB > 0 % uphill flow
            if N_lv > N_lv_bs
                flow_reg = 1; % bubble flow
            else
                flow_reg = 2; % slug flow
            end
        else % downhill or horizontal flow
            if abs(theta_MB) > pi/6 % i.e. alpha < 60 deg.
                if N_gv > N_gv_bs
                    if N_lv > N_lv_st
                        flow_reg = 2; % slug flow
                    else
                        flow_reg = 4; % stratified flow
                    end
                else
                    flow_reg = 1; % bubble flow
                end
            else % abs(theta_MB) <= pi/6, i.e. alpha >= 60 deg.
                if N_lv > N_lv_st
                    if N_gv > N_gv_bs
                        flow_reg = 2; % slug flow
                    else
                        flow_reg = 1; % bubble flow
                    end
                else
                    flow_reg = 4; % stratified flow
                end
            end
        end
    end
%     fid = fopen('flow_reg.txt','a');fwrite(fid,flow_reg);fclose(fid);
    % Compute holdup correlation parameters:
    if flow_dir == 0 || flow_dir == 1 % horizontal or uphill flow
        C1 = -0.380113;
        C2 =  0.129875;
        C3 = -0.119788;
        C4 =  2.343227;
        C5 =  0.475686;
        C6 =  0.288657;
    else % downhill flow
        if flow_reg == 4 % downhill stratified flow
            C1 = -1.330282;
            C2 = 4.808139;
            C3 = 4.171584;
            C4 = 56.262268;
            C5 = 0.079951;
            C6 = 0.504887;
        else % downhill other flow
            C1 = -0.516644;
            C2 = 0.789805;
            C3 = 0.551627;
            C4 = 15.519214;
            C5 = 0.371771;
            C6 = 0.393952;
        end
    end
```

```
    % Compute liquid and gas volume fractions (no-slip):
    lambda_l = q_l/(q_l+q_g); % liquid volume fraction, -
    lambda_g = 1-lambda_l; % gas volume fraction, -

    % Compute liquid and gas holdups (with slip):
    help08 = C1 + C2*sin(theta_MB) + C3*(sin(theta_MB))^2 + C4*N_l^2;
    help09 = N_gv^C5 / N_lv^C6;
    H_l = exp(help08*help09); % liquid hold-up, -
    if H_l < 1e-9
        H_l = 1e-9; % to avoid numerical problems and stay within look-up
table below
    end
    if H_l < lambda_l % Reality check (not included in [1] or [2])
        H_l = lambda_l;
    end
    H_g = 1-H_l; % gas hold-up, -

    % Compute 'slip' and 'no-slip' gas-liquid mixture properties:
    mu_n = mu_l*lambda_l + mu_g*lambda_g; % 'no-slip' gas-liquid mixture
                                          % viscosity, Pa s
    rho_n = rho_l*lambda_l + rho_g*lambda_g; % 'no-slip' gas-liquid mixture
                                             % density, kg/m^3
    rho_s = rho_l*H_l + rho_g*H_g; % 'slip' gas-liquid mixture density,
kg/m^3

    % Compute pressure gradient for bubble and slug flow:
    if flow_reg == 1 || flow_reg == 2
%         V_sl = num2str(v_m);
%         fid = fopen('mixture_velocity.txt','a');
%         fprintf(fid,'\t%s',V_sl);
%         fclose(fid);
        help21 = (rho_s*v_m*v_sg)/p_tot; % acceleration loss factor E_k, -
        help22 = rho_s*g*cos(alpha);
        dpds_grav = help22; % gravity losses, Pa/m
        f_r = 1; % linear interpolation of friction factor ratio(slip,no-
slip)
        % Eccentric friction loss power-law fluid Pa/m
        help23 =
powerlaw(v_m,f_r,rho_n,rho_s,dp,dc,Fannreading,ec,flow_reg);
        dpds_fric = help23; % friction losses, Pa/m
        dpds_acc = (help22+help23)*(help21/(1-help21)); % acceleration
losses,
                                                        % Pa/m
        dpds_tot = dpds_grav + dpds_fric + dpds_acc; % total pressure
gradient,
                                                        % Pa/m
        dpds = [dpds_tot;dpds_grav;dpds_fric;dpds_acc];
   end
```

```
    % Compute pressure gradient for annular flow:
    if flow_reg == 3
        H_r = lambda_l/H_l; % volume fraction - holdup ratio, -
        H_r_table_values = [1.e-9 0.01 0.20 0.30 0.40 0.50 0.70 1.00 10.00
...                          1.e9];
        f_r_table_values = [1.00  1.00 0.98 1.20 1.25 1.30 1.25 1.00  1.00
...                          1.00];
        f_r = interp1(H_r_table_values,f_r_table_values,H_r); % linear
        % interpolation of friction factor ratio(slip,no-slip)
        help11 = (rho_s*v_m*v_sg)/p_tot; % acceleration loss factor E_k, -
        help12 = rho_s*g*cos(alpha);
        % Eccentric friction loss power-law fluid Pa/m
        help13 =
powerlaw(v_m,f_r,rho_n,rho_s,dp,dc,Fannreading,ec,flow_reg);
        dpds_grav = help12; % gravity losses, Pa/m
        dpds_fric = help13; % friction losses, Pa/m
        dpds_acc = (help12+help13)*(help11/(1-help11));
% acceleration losses,Pa/m
        dpds_tot = dpds_grav + dpds_fric + dpds_acc;
% total pressure gradient,Pa/m
        dpds = [dpds_tot;dpds_grav;dpds_fric;dpds_acc];
    end

    % Compute pressure gradient for stratified flow:
    if flow_reg == 4
        % Compute delta iteratively through successive substitution:
        iter = 0; %iteration counter, -
        max_iter = 100; % maximum allowed number of iterations, -
        error_abs = 2*pi; % initial error, rad
        tol_abs = 1.e-6; % absolute convergence criterion, rad
        delta = 0.001; % initial guess, opening angle liquid layer in
                       % stratified flow, rad.
        while error_abs > tol_abs
            delta_old = delta;
            delta = 2*pi*H_l + sin(delta_old);
            error_abs = abs(delta-delta_old);
            iter = iter+1;
            if iter > max_iter
                error_abs = 0; %%% temporary fix!!!!!!!!!
%                delta
%                H_l
%                error('Error: Maximum allowed number of iterations
exceeded.')
            end
        end
```

```
% Compute geometrical parameters:
        A_g = A * H_g; % gas cross-sectional area, m^2
        A_l = A * H_l; % liquid cross-sectional area, m^2
        help31 = sin(delta);
        help32 = sin(delta/2);
        help33 = delta-help31;
        help34 = delta-2*help32;
        help35 = delta+2*help32;
        d_hg = dh*(2*pi-help33)/(2*pi-help34); % gas hydraulic diameter, m
        d_hl = dh*help33/help35; % liquid hydraulic diameter, m
        P = pi*dh; % pipe perimeter, m
        P_g = (1-delta/(2*pi))*P; % gas wetted perimeter, m
        P_l = P - P_g; % liquid wetted perimeter, m

        % Compute shear stresses:
        v_g = v_sg/H_g; % gas velocity, m/s
        v_l = v_sl/H_l; % liquid velocity, m/s
        N_Re_g = rho_g*abs(v_g)*d_hg/mu_g; % gas Reynolds number, -
        N_Re_l = rho_l*abs(v_l)*d_hl/mu_l; % liquid Reynolds number, -
        f_g = Moody_friction_factor(epsilon,N_Re_g); % gas friction factor;
        f_l = Moody_friction_factor(epsilon,N_Re_l); % liquid friction
        tau_wg = f_g*rho_g*v_g*abs(v_g)/2; % gas shear stress, N/m^2
        tau_wl = f_l*rho_l*v_l*abs(v_l)/2; % liquid shear stress, N/m^2

        % Compute pressure gradient dpds:
        help42 = (rho_g*A_g + rho_l*A_l)*g*cos(alpha);
        help43 = -(tau_wg*P_g + tau_wl*P_l);
        dpds_grav = (help42); % gravity losses, Pa/m
        dpds_fric = (help43); % friction losses, Pa/m
        dpds_acc = 0; % acceleration losses neglected, Pa/m
        dpds_tot = dpds_grav + dpds_fric; % total pressure gradient, Pa/m
        dpds = [dpds_tot;dpds_grav;dpds_fric;dpds_acc];
    end
end
```

Subsidiary scripts:

```
function dpds_fric_ec =
powerlaw(v_m,f_r,rho_n,rho_s,dp,dc,Fannreading,ec,flow_reg)
% v = velocity of the mixture
% rho = density of the mixture
% dp = outer diameter of the drillpipe
% dc = inner diameter of the casing/borehole wall
% n_power = flow behaviour index
% ec = degree of eccentricity
% K = consistency index

% References:
% [1] Multiphase flow in Wells by J.P. Brill and H. Mukherjee,
% [2] Advanced drilling and Well technology by B.S. Aadnoy et al.

% Finding Power law values
[n,K]=Fann(Fannreading); % Power-law indices
k = dp/dc; % annulus pipe diameter ratio

%check validation
if (n<0.4 || n>=1) || (ec>=0.95 || ec<=0) || (k<=0.3 || k>=0.8)
    warning('Powerlaw model not valid')
end
```

```
% Equations for regression coefficients
A0=-2.8771*k^2-(0.1029*k)+2.6581;
A1=2.8156*k^2+(3.6114*k)-4.9072;
A2=0.7444*k^2-(4.8048*k)+2.2764;
A3=-0.3939*k^2+(0.7211*k)+0.1503;
a0=3.0422*k^2+(2.4049*k)-3.1931;
a1=-2.7817*k^2-(7.9865*k)+5.8970;
a2=-0.3406*k^2+(6.0164*k)-3.3614;
a3=0.25*k^2-(0.5780*k)+1.3591;

% Define geometric parameters a & b
a=A0*ec^3+A1*ec^2+A2*ec+A3;
b=a0*ec^3+a1*ec^2+a2*ec+a3;

Dhyd=(dc^2-dp^2)/(dc-dp); % hydraulic diameter
shear_rate_avg=((a/n)+b)*((8*abs(v_m))/Dhyd); % Average shear rate
Nre_ec=(8*rho_n*abs(v_m)^2)/(K*shear_rate_avg^n); %
K_cons= K*((4*n+2)/4*n)^n; % generalized consistency index
Nre = (rho_n*abs(v_m)^(2-n)*(dc-dp)^n)/(8^(n-1)*K_cons); % Generalized
Reynolds number
% NRE = num2str(Nre);
% fid = fopen('Nre.txt','a');
% fprintf(fid,'\t%s',NRE);
% fclose(fid);
f = 16/Nre;
f = f*f_r;
if flow_reg == 3
    dpds_fric_con = (2*-f*rho_n*v_m*abs(v_m))/(dc-dp);
end
if flow_reg == 2 || 1
    dpds_fric_con = (2*-f*rho_s*v_m*abs(v_m))/(dc-dp);
end
if flow_reg == 0
    dpds_fric_con = (2*-f*rho_n*v_m*abs(v_m))/(dc-dp);
end
if Nre_ec<2100 % laminar flow
R = 1-(0.072*(ec/n)*k^0.8454)-
(1.5*ec^2*sqrt(n)*k^0.1852)+(0.96*ec^3*sqrt(n)*k^0.2527); % Multiphase flow
in wells, Brill & Mukherjee page 11-13
dpds_fric_ec=dpds_fric_con*R;
else % turbulent flow
R = 1-(0.048*(ec/n)*k^0.8454)-
(0.67*ec^2*sqrt(n)*k^0.1852)+(0.28*ec^3*sqrt(n)*k^0.2527); % Advanced
drilling and Well technology, Aadnoy et al. page 216-217
dpds_fric_ec=dpds_fric_con*R;
end
```

```
function [Vt,percentage_solid] =
per_solid_in_mudvolume(q_sc,p_wf,T_wf,dc,ROP,rho_sc)

T=T_wf;
% flow rates at standard conditions:
q_g_sc = q_sc(1); % gas flow rate at standard conditions, m3/s
q_o_sc = q_sc(2); % oil flow rate at standard conditions, m3/s

% Compute local gas and liquid properties:
R_go = q_g_sc/q_o_sc; % producing GOR as would be observed at surface,
m^3/m^3
R_sb = R_go; % This is the bubble point GOR for the oil in the wellbore.
This
             % value may be much higher than R_sb in the reservoir if gas-
cap gas
             % or lift gas is produced.
q = local_q_and_rho(p_wf,q_sc,R_sb,rho_sc,T);
if q_o_sc ~= 0 % Check wether mud is made up of water or oil
    q_bottomhole = abs(q(2)); % Mud volume rate at the bottom of the well
else
    q_bottomhole = abs(q(3)); % Mud volume rate at the bottom of the well
end
% Amount of cuttings that get liberated and dissolved(97%)
rock_volume = (pi*dc^2)/4*(ROP/60)*0.97;
Vt = q_bottomhole + rock_volume;
percentage_solid = (rock_volume/Vt)*100;
```

```
function [n,K]=Fann(Fannreading)

% Fannreading must be a vector with 6 numbers
% RPM = Rounds per Minute
% K = Consistency index
% n = Flow behaviour index

% Reference:
% Drilling fluids processing handbook page 36-37, author: ASME
% Publisher: Elsevier

RPM=[3 6 100 200 300 600];
%% Power law indices from nonlinear regression
c = polyfit(log(RPM*1.703),log(Fannreading*5.11e-1),1); % Least square
solution
K = exp(c(2));
n = c(1);
```

```
function [B_g,B_o,R_s] = black_oil_Standing(p,R_sb,rho_g_sc,rho_o_sc,T)
% [B_g,B_o,R_s] = black_oil_Standing(p,R_sb,rho_g_sc,rho_o_sc,T)
%
% Computes the gas and oil formation volume factors B_g and B_o and the
% solution GOR R_s at a given pressure p and temperature T, bubble point
GOR R_sb,
% and gas and oil densities rho_g_sc and rho_o_sc. The pressure p may be
% below or above the bubble point pressure.
%
% For the oil parameters p_b, B_o and R_s, use is made of the Standing
correlations,while for compressibility c_o and modified gas density
rho_g_100, we used the Vazquez and Beggs correlations.
%
% To compute the gas parameter B_g, use is made of the Sutton correlations
for pseudo-critical pressure p_pc and temperature T_pc, and of the Dranchuk
and Abu-Kassem approximation of the Standing-Katz correlation for the Z
factor.
% B_g = gas-formation volume factor, m^3/m^3
% B_o = oil-formation volume factor, m^3/m^3
% p = pressure, Pa
% R_sb = solution gas-oil ratio at bubble point pressure, m^3/m^3
% R_s = solution gas-oil ratio, m^3/m^3
% rho_g_sc = gas density at standard conditions, kg/m^3
% rho_o_sc = oil density at standard conditions, kg/m^3
% T = temperature, deg. C
%
% Reference: AES1360 Production Optimisation, TU Delft

% Standard conditions:
p_sc = 100e3; % pressure at standard conditions, Pa
T_sc = 15; % temperature at standard conditions, deg. C

p_b = pres_bub_Standing(R_sb,rho_g_sc,rho_o_sc,T); % bubble point pressure,
Pa

% Oil parameters:
if p <= p_b % saturated oil
    R_s = gas_oil_rat_Standing(p,rho_g_sc,rho_o_sc,T);
    B_o = oil_form_vol_fact_Standing(R_s,rho_g_sc,rho_o_sc,T);
else % undersaturated oil
    R_s = R_sb;
    B_ob = oil_form_vol_fact_Standing(R_s,rho_g_sc,rho_o_sc,T); % oil
formation volume factor at bubble point pressure, m^3/m^3
    rho_g_100 = rho_g_Vazquez_and_Beggs(p_sc,rho_g_sc,rho_o_sc,T_sc); % gas
density at 100 psi, kg/m^3
    c_o = compres_Vazquez_and_Beggs(p,R_s,rho_g_100,rho_o_sc,T); % oil
compressibility, 1/Pa
    B_o = oil_form_vol_fact_undersat(B_ob,c_o,p,p_b);
end
% Gas parameter:
T_abs = T + 273.15; % absolute temperature, K
p_pc = pres_pseu_crit_Sutton(rho_g_sc); % pseudo-critical pressure, Pa
T_pc = temp_pseu_crit_Sutton(rho_g_sc); % pseudo-critical temperature, K
p_pr = p / p_pc; % pseudo-reduced pressure, -
T_pr = T_abs / T_pc; % pseudo reduced temperature, -
Z = Z_factor_DAK(p_pr,T_pr); % Z factor, -
B_g = gas_form_vol_fact(p,T_abs,Z);
```

```
function [q,rho] = local_q_and_rho(p,q_sc,R_sb,rho_sc,T)
% [q,rho] = local_q_and_rho(p,q_sc,R_sb,rho_sc,T)
%
% Computes the local values of q = [q_g,q_o,q_w] and rho =
[rho_g,rho_o,rho_w]
% from q_sc = [q_g_sc,q_o_sc,q_w_sc]
% rho_sc = [rho_g_sc,rho_o_sc,rho_w_sc]
% at a given pressure p, temperature T and bubble point GOR R_sb.
%
% p = pressure, Pa
% q = [q_g,q_o,q_w]
% q_g = gas flow rate at local conditions, m^3/s
% q_o = oil flow rate at local conditions, m^3/s
% q_w = water flow rate at local conditions, m^3/s
% q_sc = [q_g_sc,q_o_sc,q_w_sc]
% q_g_sc = gas flow rate at standard conditions, m^3/s
% q_o_sc = oil flow rate at standard conditions, m^3/s
% q_w_sc = water flow rate at standard conditions, m^3/s
% R_sb = gas-oil ratio at bubble point pressure, m^3/m^3
% rho = [rho_g,rho_o,rho_w]
% rho_g = gas density at local conditions, kg/m^3
% rho_o = oil density at local conditions, kg/m^3
% rho_w = water density at local conditions, kg/m^3
% rho_sc = [rho_g_sc,rho_o_sc,rho_w_sc]
% rho_g_sc = gas density at standard conditions, kg/m^3
% rho_o_sc = oil density at standard conditions, kg/m^3
% rho_w_sc = water density at standard conditions, kg/m^3
% T = temperature, deg. C
%
% Reference: AES1360 Production Optimisation, TU Delft

% Compute black-oil parameters:
% B_g = gas-formation volume factor, m^3/m^3
% B_o = oil-formation volume factor, m^3/m^3
% R_s = solution gas-oil ratio, m^3/m^3
rho_g_sc = rho_sc(1);
rho_o_sc = rho_sc(2);
[B_g,B_o,R_s] = black_oil_Standing(p,R_sb,rho_g_sc,rho_o_sc,T);
% Assemble transformation matrices T_q and T_rho:
T_q(1,1) =  B_g;
T_q(1,2) = -B_g*R_s;
T_q(1,3) =  0;
T_q(2,1) =  0;
T_q(2,2) =  B_o;
T_q(2,3) =  0;
T_q(3,1) =  0;
T_q(3,2) =  0;
T_q(3,3) =  1;

T_rho(1,1) =  1/B_g;
T_rho(1,2) =  0;
T_rho(1,3) =  0;
T_rho(2,1) =  R_s/B_o;
T_rho(2,2) =  1/B_o;
T_rho(2,3) =  0;
T_rho(3,1) =  0;
T_rho(3,2) =  0;
T_rho(3,3) =  1;
% Compute local values:
q = T_q*q_sc';
rho = T_rho*rho_sc';
```

```
function c_o = compres_Vazquez_and_Beggs(p,R_sb,rho_g_100,rho_o_sc,T)
% c_o = compres_Vazquez_and_Beggs(p,R_sb,rho_g_100,rho_o_sc,T)
%
% Computes the compressibility with the Vazquez and Beggs correlation
converted to SI units.
%
% c_o = oil compressibility, 1/Pa
% p = pressure, Pa
% R_sb = solution gas oil ratio at bubble point pressure, m^3/m^3
% rho_g_100 = gas density at 100 psig, kg/m^3
% rho_o_sc = oil density at standard conditions, kg/m^3
% T = temperature, deg. C
%
% Reference: AES1360 Production Optimisation, TU Delft

help01 = 27.8 * R_sb;
help02 = 31 * T;
help03 = 959 * rho_g_100;
help04 = 1784000/rho_o_sc;
c_o = (-2541 + help01 + help02 - help03 + help04) / (1e5*p);
```

```
function B_g = gas_form_vol_fact(p,T_abs,Z)
% B_g = gas_form_vol_fact(p,T_abs,Z)
%
% Computes the gas formation volume factor in SI units.
%
% B_g = gas formation volume factor m^3/m^3
% p = presssure, Pa
% T = temperature, K
% Z = gas compressibility factor, -
%
% Reference: AES1360 Production Optimisation, TU Delft

p_sc = 100e3; % pressure at standard conditions, Pa
T_sc_abs = 15 + 273.15; % temperature at standard conditions, K
Z_sc = 1; % gas compressibility factor at standard conditions, -
B_g = (p_sc * T_abs * Z) / (p * T_sc_abs * Z_sc);
```

```
function R_s = gas_oil_rat_Standing(p,rho_g_sc,rho_o_sc,T)
% R_s = gas_oil_rat_Standing(p,rho_g_sc,rho_o_sc,T)
%
% Computes the solution gas-oil ratio with a Standing correlation converted
to
% SI units.
%
% R_s = solution gas-oil ratio, m^3/m^3
% p = pressure, Pa
% rho_g_sc, gas density at standard conditions, kg/m^3
% rho_o_sc, oil density at standard conditions, kg/m^3
% T = temperature, deg. C
%
% Reference: AES1360 Production Optimisation, TU Delft

help01 = 10^(1768/rho_o_sc - 0.00164*T);
R_s = (rho_g_sc/716)*((8e-6*p+1.4)*help01)^1.2048;
```

```
function mu_g_p_sc = gas_visc_atm_Dempsey(M,T)
% mu_g_p_sc = gas_visc_atm_Dempsey(M,T)
%
% Calculates the gas viscosity at atmosperic pressure as a function of
% molar mass M and temperature T in SI units
%
% Use is made of an expression of Dempsey (1965) to approximate the
correlation
% of Carr, Kobayashi and Burrows (1954).
%
% M = molar mass, kg/kmol
% mu_g_p_sc = viscosity at atmospheric pressure, Pa s
% T = temperature, deg. C
%
% Reference: AES1360 Production Optimisation, TU Delft

b0 =  1.16620808E-05;
b1 =  3.04342760E-08;
b2 =  6.84808007E-12;
b3 = -1.11626158E-07;
b4 = -1.25617746E-10;
b5 = -2.91397349E-13;
b6 =  4.64955375E-10;
b7 =  4.29044857E-13;
b8 =  1.28865249E-15;

mu_g_p_sc = b0 + b1*T + b2*T^2 + b3*M + b4*T*M + b5*T^2*M + b6*M^2 +
b7*T*M^2 + b8*T^2*M^2;
```

```
function mu_g = gas_viscosity(p,rho_g_sc,T)
% mu_g = gas_viscosity(p,rho_g_sc,T)
%
% Calculates the gas viscosity as a function of pressure, temperature and
% gas density at standard conditions in SI units.
%
% Use is made of the Dempsey (1965) approximations of the Carr, Kobayashi
% and Burrows (1954) correlations.
%
% mu_g = gas viscosity, Pa s
% p = pressure, Pa
% rho_g_sc = gas density at standard condition, kg/m^3
% T = temperature, deg. C
%
% Reference: AES1360 Production Optimisation, TU Delft

M = from_kg_per_m3_to_molar_mass(rho_g_sc); % molar mass, kg/kmol
mu_g_p_sc = gas_visc_atm_Dempsey(M,T); % gas viscosity at atmospheric
pressure, Pa s
p_pc = pres_pseu_crit_Sutton(rho_g_sc); % pseudo-critical pressure, Pa
T_pc = temp_pseu_crit_Sutton(rho_g_sc); % pseudo-critical temperature, K
p_pr = p/p_pc; % pseudo-reduced pressure, -
T_abs = T + 273.15; % absolute temperature, K
T_pr = T_abs/T_pc; % pseudo-reduced temperature, -
f = gas_visc_ratio_Dempsey(p_pr,T_pr); % gas viscosity ratio, -
mu_g = f * mu_g_p_sc;
```

```
function f = gas_visc_ratio_Dempsey(p_pr,T_pr)
% f = gas_visc_ratio_Dempsey(p_pr,T_pr)
%
% Calculates the ratio f between the gas viscosity at any pressure and the
viscosity
% at atmosperic pressure for a given pseudo-reduced pressure and
temperature.
%
% Use is made of an expression of Dempsey (1965) to approximate the
correlation
% of Carr, Kobayashi and Burrows (1954).
%
% f = gas viscosity ratio = mu_g / mu_g_p_sc, -
% p_pr = pseudo-reduced pressure, -
% T_pr = pseudo-reduced temperature, -
%
% Reference: AES1360 Production Optimisation, TU Delft

 a0 = -2.46211820e-00;
 a1 =  2.97054714e-00;
 a2 = -2.86264054e-01;
 a3 =  8.05420522e-03;
 a4 =  2.80860949e-00;
 a5 = -3.49803305e-00;
 a6 =  3.60373020e-01;
 a7 = -1.04432413e-02;
 a8 = -7.93385684e-01;
 a9 =  1.39643306e-00;
a10 = -1.49144925e-01;
a11 =  4.41015512e-03;
a12 =  8.39387178e-02;
a13 = -1.86408848e-01;
a14 =  2.03367881e-02;
a15 = -6.09579263e-04;

help01 =           a0 +  a1*p_pr +  a2*p_pr^2 +  a3*p_pr^3 ;
help02 = T_pr   * ( a4 +  a5*p_pr +  a6*p_pr^2 +  a7*p_pr^3);
help03 = T_pr^2 * ( a8 +  a9*p_pr + a10*p_pr^2 + a11*p_pr^3);
help04 = T_pr^3 * (a12 + a13*p_pr + a14*p_pr^2 + a15*p_pr^3);

f = exp(help01+help02+help03+help04) / T_pr;
```

```
function sigma = interfacial_tensions()
% sigma = interfacial_tensions()
%
% Input function for interfacial tensions
%
% Reference: AES1360 Production Optimisation, TU Delft

sigma_go = 0.008; % gas-oil interfacial tension, N/m
sigma_gw = 0.04; % gas-water interfacial tension, N/m
sigma = [sigma_go,sigma_gw];
```

```
function B_o = oil_form_vol_fact_Standing(R_s,rho_g_sc,rho_o_sc,T)
% B_o = oil_form_vol_fact_Standing(R_s,rho_g_sc,rho_o_sc,T)
%
% Computes the oil formation volume factor with a Standing correlation
converted to SI units.
%
% B_o = oil formation volume factor, m^3/m^3
% R_s = solution gas-oil ratio, m^3/m^3
% rho_g_sc = gas density at standard conditions, kg/m^3
% rho_o_sc = oil density at standard conditions, kg/m^3
% T = temperature, deg. C
%
% Reference: AES1360 Production Optimisation, TU Delft

help01 = sqrt(rho_g_sc/rho_o_sc);
B_o = 0.9759 + 12e-5 *(160 * R_s * help01 + 2.25 * T + 40)^1.2;
```

```
function B_o = oil_form_vol_fact_undersat(B_ob,c_o,p,p_b)
% B_o = oil_form_vol_fact_undersat(B_ob,c_o,p,p_b)
%
% Computes the oil formation volume factor for undersaturated oil.
% Valid for SI units and field units.
%
% B_o = oil formation volume factor, m^3/m^3, (bbl/bbl)
% B_ob = oil formation volume factor at bubble point pressure,
%        m^3/m^3, (bbl/bbl)
% c_o = compressibility, 1/Pa, (1/psi)
% p = presssure, Pa, (psi)
% p_b = bubble point pressure, Pa, (psi)
%
% Reference: AES1360 Production Optimisation, TU Delft

B_o = B_ob * exp(-c_o*(p - p_b));
```

```
function mu_od = oil_visc_dead_B_and_R(rho_o_sc,T)
% mu_od = oil_visc_dead_B_and_R(rho_o_sc,T)
%
% Computes the dead-oil viscosity using the Beggs and Robinson correlation
% in SI units.
%
% mu_od = dead-oil viscosity, Pa s
% rho_o_sc = oil density at standard conditions, kg/m^3
% T = temperature, C
%
% Reference: AES1360 Production Optimisation, TU Delft

b = 5.693-2.863*10^3/rho_o_sc;
a = 10^b / (1.8*T+32)^1.163;
mu_od = 10^-3*(10^a-1);
```

```
function mu_o = oil_visc_sat_B_and_R(mu_od,R_s)
% mu_o = oil_visc_sat_B_and_R(mu_od,R_s)
%
% Computes the saturated-oil viscosity using the Beggs and Robinson
correlation
% in SI units.
%
% mu_o = saturated-oil viscosity, Pa s
% mu_od = dead-oil viscosity, Pa s
% R_s = solution gas-oil ratio, m^3/m^3
%
% Reference: AES1360 Production Optimisation, TU Delft

c = 3.04*(R_s+26.7)^-0.338;
mu_o = (4.4065*(R_s+17.8)^-0.515)*mu_od^c;
```

```
function mu_o = oil_visc_undersat_V_and_B(mu_ob,p,p_b)
% mu_o = oil_visc_undersat_V_and_B(mu_ob,p,p_b)
%
% Computes the undersaturated-oil viscosity using the Vazquez and Beggs
correlation
% in SI units.
%
% mu_o = undersaturated-oil viscosity, Pa s
% mu_ob = oil viscosity at bubble point, Pa s
% p = pressure, Pa
% p_b = bubble point pressure, Pa
%
% Reference: AES1360 Production Optimisation, TU Delft

d = 7.2e-5*p^1.187*exp(-11.513-1.30e-8*p);
mu_o = mu_ob*(p/p_b)^d;
```

```
function p_pc = pres_pseu_crit_Sutton(rho_g_sc)
% p_pc = pres_pseu_crit_Sutton(rho_g_sc)
%
% Calculates the pseudo-critical pressure of a gas mixture
% with unknown composition, using the Sutton (1985) correlation
% converted to SI units.
%
% p_pc = pseudo-critical pressure, Pa
% rho_g_sc = gas density at standard conditions, kg/m^3
%
% valid for rho_g_sc < 6.24 kg/m3
% Reference: AES1360 Production Optimisation, TU Delft

p_pc = 5218e3 - 734e3 * rho_g_sc - 16.4e3 * rho_g_sc^2;
```

```
function mu_o = oil_viscosity(p,R_sb,rho_g_sc,rho_o_sc,T)
% mu_o = oil_viscosity(p,R_sb,rho_g_sc,rho_o_sc,T)
%
% Computes the oil viscosity at given pressure, temperature,
% producing GOR and oil and gas densities at standard conditions.
% The pressure may be below or above the bubble point pressure.
%
% For the dead-oil viscosity and the saturated-oil viscosity use is made of
% the Beggs and Robinson(1975) correlations, while for the undersaturated-
oil
% viscosity we used the Vazquez and Beggs (1980) correlation. For the black
oil
% properties we use the Standing (1952) correlations.
%
% mu_o = oil viscosity, Pa s
% p = pressure, Pa
% rho_g_sc = gas density at standard conditions, kg/m^3
% rho_o_sc = oil density at standard conditions, kg/m^3
% R_sb = gas-oil ratio at bubble point pressure, m^3/m^3
% T = temperature, deg. C
%
% Reference: AES1360 Production Optimisation, TU Delft

% Dead-oil viscosity:
mu_od = oil_visc_dead_B_and_R(rho_o_sc,T);

% Black oil properties:
p_b = pres_bub_Standing(R_sb,rho_g_sc,rho_o_sc,T); % bubble point pressure,
Pa

% Oil viscosity:
if p<p_b
   R_s = gas_oil_rat_Standing(p,rho_g_sc,rho_o_sc,T); % solution gas-oil
ratio, m^3/m^3
   mu_o = oil_visc_sat_B_and_R(mu_od,R_s); % saturated oil viscosity, Pa s
else
   mu_ob = oil_visc_sat_B_and_R(mu_od,R_sb); % oil viscosity at bubble
point, Pa s
   mu_o = oil_visc_undersat_V_and_B(mu_ob,p,p_b); % undersaturated oil
viscosity, Pa s
end
```

```
function T_pc = temp_pseu_crit_Sutton(rho_g_sc)
% T_pc = temp_pseu_crit_Sutton(rho_g_sc)
%
% Calculates the pseudo-critical temperature of a gas mixture
% with unknown composition, using the Sutton (1985) correlation
% converted to SI units.
%
% rho_g_sc, gas density at standard conditions, kg/m^3
% T_pc = pseudo-critical temperature, K
%
% Reference: AES1360 Production Optimisation, TU Delft
%
T_pc = 94.0 + 157.9 * rho_g_sc - 27.2 * rho_g_sc^2;
```

```
function p_b = pres_bub_Standing(R_sb,rho_g_sc,rho_o_sc,T)
% p_b = pres_bub_Standing(R_sb,rho_g_sc,rho_o_sc,T)
%
% Computes the bubble point pressure with a Standing correlation converted
% to SI units.
%
% R_sb = gas-oil ratio at bubble point pressure, m^3/m^3
% p_b = bubble point pressure, Pa
% rho_g_sc = gas density at standard conditions, kg/m3
% rho_o_sc = oil density at standard conditions, kg/m3
% T = temperature, deg. C
%
% Reference: AES1360 Production Optimisation, TU Delft

% check for presence of gas:
if rho_g_sc == 0
    p_b = 1.e5; % atmospheric pressure
else
    help01 = (10^(0.00164*T))/(10^(1768/rho_o_sc));
    p_b = 125e3 * ((716*R_sb/rho_g_sc)^0.83 * help01 - 1.4);
end

% Reality check:
if p_b < 1.e5
    p_b = 1.e5; % atmospheric pressure
end
```

```
function rho_g_100 =
rho_g_Vazquez_and_Beggs(p_sep,rho_g_sep,rho_o_sc,T_sep)
% rho_g_100 = rho_g_Vazquez_and_Beggs(p_sep,rho_g_sep,rho_o_sc,T_sep)
%
% Computes the equivalent gas density as if determined from a sample taken
at a separator
% pressure of 689 kPa (100 psi). Input is the gas density rho_g determined
from a sample
% taken at another (separator) pressure p_sep and temperature T_sep. Use is
made of a
% correlation from Vazquez and Beggs, converted to SI units.
%
% p_sep = separator pressure, Pa
% rho_g_sep = gas density at p_sep, kg/m^3
% rho_g_100 = gas density at 100 psi, kg/m^3
% rho_o_sc = oil density at standard conditions, kg/m^3
% T_sep = separator temperature, deg. C
%
% Reference: AES1360 Production Optimisation, TU Delft

help01 = 141500 / rho_o_sc - 131.5;
help02 = 1.8 * T_sep + 32;
help03 = p_sep /790.8e3;
rho_g_100 = rho_g_sep * (1 + 5.912e-5 * help01 * help02 * log10(help03));
```

```
function mu_w = water_viscosity()
% mu_w = water_viscosity()
%
% Input function for water viscosity
%
% Reference: AES1360 Production Optimisation, TU Delft

mu_w = 0.35e-3; % water viscosity (taken as viscosity at 50 deg. C), Pa s
```

```
function Z = Z_factor_DAK(p_pr,T_pr)
% Z = Z_factor_DAK(p_pr,T_pr)
%
% Calculates the Z-factor for a given reduced pressure and reduced
temperature.
% Use is made of the correlation of Dranchuk & Abu-Kasem (1975) to
approximate the
% Standing & Katz (1942) chart.
%
% The range of validity for the approximation is
% 0.2 < p_pr < 30 and 1.0 < T_pr < 3.0 .
%
% Z = Z factor, -
% p_pr = pseudo-reduced pressure, -
% T_pr = pseudo-reduced temperature, -
%
% Reference: AES1360 Production Optimisation, TU Delft

a1 =  0.3265;
a2 = -1.0700;
a3 = -0.5339;
a4 =  0.01569;
a5 = -0.05165;
a6 =  0.5475;
a7 = -0.7361;
a8 =  0.1844;
a9 =  0.1056;
a10 = 0.6134;
a11 = 0.7210;

c = 0.27 * p_pr/T_pr;

b1 = c * (a1 + a2/T_pr + a3/T_pr^3 + a4/T_pr^4 + a5/T_pr^5);
b2 = c^2 * (a6 + a7/T_pr + a8/T_pr^2);
b3 = c^5 * a9*(a7/T_pr + a8/T_pr^2);
b4 = c^2 * a10/T_pr^3;
b5 = c^2 * a11;
b6 = b4 * b5;

% Initiate Z with the Papay correlation:
Z_0 = 1 - 3.52*p_pr/(T_pr*10^0.9813) + 0.274*p_pr^2/(T_pr*10^0.8157) ;
Z = Z_0;

% Improve the result with Newton Raphson iteration:
tol_abs = 1.e-8; % Absolute convergence criterion
tol_rel = 1.e-9; % Relative convergence criterion
max_iter = 100; % Maximum allowed number of iterations
max_diff = 0.5; % Maximum allowed absolute difference in Z per iteration
step
```

```
iter = 0; % Iteration counter
repeat = 1;
while repeat > 0
   if iter > max_iter
      p_pr
      T_pr
      Z_0
      Z
      error('Error: Maximum allowed number of iterations exceeded in
Z_factor_DAK.')
   end
   iter = iter+1;
   Z_old = Z;

   help01 = Z_old - b1*Z_old^-1 - b2*Z_old^-2 + b3*Z_old^-5;
   help02 = -(b4*Z_old^-2 + b6*Z_old^-4) * exp(-b5*Z_old^-2) - 1;
   fZ = help01 + help02;

   help03 = 1 + b1*Z_old^-2 + 2*b2*Z_old^-3 - 5*b3*Z_old^-6;
   help04 = (2*b4*Z_old^-3 - 2*b4*b5*Z_old^-5 + 4*b6*Z_old^-5 -
2*b5*b6*Z_old^-7) * exp(-b5*Z_old^-2);
   dfZdZ = help03 + help04;

   Z = Z_old - fZ/dfZdZ; % Newton Raphson iteration
   diff = Z-Z_old;
   if abs(diff) > max_diff % Check if steps are too large
      Z = Z_old + max_diff * sign(diff); % Newton Raphson iteration with
reduced step size
      diff = max_diff;
   end
   rel_diff = diff/Z_old;
   if abs(diff) > tol_abs % Check for convergence
      repeat = 1;
   else
      if abs(rel_diff) > tol_rel
         repeat = 1;
      else
         repeat = 0;
      end
   end
end
```

```
function f = Moody_friction_factor(epsilon,N_Re)
% f = Moody_friction_factor(epsilon,N_Re)
%
% Computes the friction factor for pipe flow according to the Moody (1944)
diagram.
% In the turbulent region, the implicit Colebrook (1939) expression is used
to
% compute the friction factor iteratively via subsequent substitution.
%
% epsilon = dimensionless roughness, -
% f = friction factor, -
% N_Re = Reynolds number, -
%
% Reference: AES1360 Production Optimisation, TU Delft

if N_Re < 2000 % Laminar regime
   f = 64/N_Re;
```

```
else % Turbulent or transitional regime
   if N_Re < 3000 % Transitional regime: prepare for interpolation
      f_lam_max = 64/2000; % Highest laminar value
      alpha = (N_Re-2000)/(3000-2000); % Interpolation parameter
      N_Re_work = 3000; % Set N_Re_work to compute lowest turbulent value
   else % Turbulent regime
      N_Re_work = N_Re;
   end
   % Initialize f_work with the Zigrang and Sylvester (1985) approximation
   % for the Colebrook (1939) friction factor:
   help01 = 2*epsilon/3.7 + 13/N_Re_work;
   help02 = (5.02/N_Re_work)*log10(help01);
   f_work = 1/(-2*log10(2*epsilon/3.7 - help02))^2;

   % Improve the result through iteration:
    tol_abs = 1.e-9; % Absolute convergence criterion
    tol_rel = 1.e-8; % Relative convergence criterion
    max_iter = 100; % Maximum allowed number of iterations
    iter = 0; % Iteration counter
    repeat = 1;
    while repeat > 0
    if iter > max_iter
          error('Error: Maximum allowed number of iterations exceeded in 
Moody_friction_factor.')
    end
       iter = iter+1;
    f_old = f_work;

      % Improve the estimate:
      help03 = 18.7/(N_Re_work*sqrt(f_old));
    f_work = 1/(1.74 - 2*log10(2*epsilon + help03))^2;

    % Check for convergence:
    diff = f_work-f_old;
    rel_diff = diff/f_old;
    if abs(diff) > tol_abs % Check for convergence
        repeat = 1;
    else
        if abs(rel_diff) > tol_rel
            repeat = 1;
        else
            repeat = 0;
        end
    end
    end

   if N_Re < 3000 % Transitional regime: interpolate between
                  % highest laminar and lowest turbulent values
      f_turb_min = f_work;
      f = f_lam_max + alpha * (f_turb_min - f_lam_max);
   else % Turbulent regime
      f = f_work;
   end
end
```

Excel sheet sensitivity analysis:

Sensitivity analysis Bachelorproject

	Lowest value		Average value		Highest value	Unit	Note
Ec	0,5	0,6	0,75	0,85	0.9	-	Eccentricity range [0-0.95]
GOR	1	1,5	2	3	4	-	Gas to Oil ratio
qo/qw	2000	2100	2200	2300	2400	l/min	Pumprate
BHT @ 3km	80	85	90	100	120	celcius	Temperature at bottom of the well
Rho_o	840	850	860	870	880	kg/m3	Density of oil-base mud
Rho_g	0,668	0,85	0,95	1,25	1,5	Kg/m3	Density of gas in the gasreservoir
Rho_w	1000	1025	1050	1100	1200	kg/m3	Density of water-base mud

Result **WBM**

	Low		Avg		High
GOR	3,98E+06	3,98E+06	3,98E+06	3,99E+06	4,00E+06
BHT	3,98E+06	3,98E+06	3,98E+06	3,98E+06	3,99E+06
rho_w	3,98E+06	3,98E+06	3,98E+06	3,99E+06	3,99E+06
rho_g	3,99E+06	3,98E+06	3,98E+06	3,98E+06	3,98E+06
qw	3,84E+06	3,91E+06	3,98E+06	4,06E+06	4,13E+06

Result **OBM**

	Low		Avg		High
GOR	4,02E+06	4,02E+06	4,02E+06	4,03E+06	4,03E+06
BHT	4,02E+06	4,02E+06	4,02E+06	4,03E+06	4,04E+06
rho_g	4,02E+06	4,02E+06	4,02E+06	4,03E+06	4,03E+06
rho_o	4,02E+06	4,02E+06	4,02E+06	4,02E+06	4,02E+06
qo	3,87E+06	3,95E+06	4,02E+06	4,10E+06	4,17E+06

WBM(fractions)

	Low		Avg		High
GOR	-0,0016	-0,0008	0,0000	0,0016	0,0032
BHT	-0,0001	0,0000	0,0000	0,0001	0,0002
rho_w	-0,0001	-0,0001	0,0000	0,0002	0,0008
rho_g	0,0003	0,0001	0,0000	-0,0002	-0,0003
qw	-0,0374	-0,0184	0,0000	0,0179	0,0354

OBM(fractions)

	low		Avg		High
GOR	-0,0007397	-0,0003703	0	0,0007439	0,0014922
BHT	-0,0011762	-0,0005903	0	0,0011929	0,0036227
rho_g	-0,0012035	-0,0004244	0	0,0012591	0,0022946
rho_o	-0,0002239	-0,0001105	0	0,0001078	0,0002129
qo	-0,0374071	-0,0184363	0	0,01794	0,0354179

Result

	-20%	-10%	0%	10%	20%
n	4,02E+06	5,32E+06	7,08E+06	9,51E+06	1,28E+07
K	5,67E+06	6,38E+06	7,08E+06	7,79E+06	8,50E+06
Ec	4,55E+06	4,28E+06	4,02E+06	3,79E+06	3,60E+06

Fracties

	-20%	-10%	0%	10%	20%
n	-0,43	-0,25	0,00	0,34	0,81
K	-0,20	-0,10	0,00	0,10	0,20
Ec	0,13	0,06	0,00	-0,06	-0,11